
Masters

Science

2006-01-01

Electronic and Optical Processes in Fullerene Films

Naomi Brant

Technological University Dublin, Naomi.Brant@tudublin.ie

Follow this and additional works at: <https://arrow.tudublin.ie/scienmas>



Part of the [Physics Commons](#)

Recommended Citation

Brant, N. (2006). *Electronic and optical processes in Fullerene films*. Masters dissertation. Technological University Dublin. doi:10.21427/D75K6W.

This Theses, Masters is brought to you for free and open access by the Science at ARROW@TU Dublin. It has been accepted for inclusion in Masters by an authorized administrator of ARROW@TU Dublin. For more information, please contact yvonne.desmond@tudublin.ie, arrow.admin@tudublin.ie, brian.widdis@tudublin.ie.



This work is licensed under a [Creative Commons Attribution-NonCommercial-Share Alike 3.0 License](#)



School of Physics/FOCAS,
Dublin Institute of Technology
Kevin Street,
Dublin 8.

Electronic and optical processes in Fullerene thin films

By

Naomi Brant BSc

A thesis submitted to the Dublin Institute of Technology,
For the degree of Master of Philosophy (MPhil)

2006

Supervisor: Dr. Hugh J. Byrne

Acknowledgements

There are many people that I would like to thank. First and foremost is my supervisor Dr. Hugh Byrne, whose kindness and encouragement has helped me throughout my research. With his enthusiasm, his inspiration, and his great efforts to explain things clearly and simply, he helped to make this a fun and rewarding experience for me. Throughout my thesis-writing period, he provided encouragement, sound advice, good teaching and lots of good ideas. I would have been lost without him and I owe him a great deal for his constructive suggestions and ideas.

I wish to thank my friends, Jennifer McCartin and Barbara O'Connell, for helping me get through the difficult times, and for all the emotional support, camaraderie, entertainment, and caring they provided.

I know this may sound strange but I would also like to thank my secondary school physics teacher Mr Tony O'Reilly whose passion and love of physics motivated me to go on and study physics at a higher level. Thanks to my brother and sisters for listening to my constant complaints throughout the years and encouraging me to never give up.

I also wish to thank my boyfriend, Luke O'Neill, you are my rock and without you I would have been lost.

Lastly, and most importantly, I wish to thank my parents, they brought me into this world, raised me, supported me, taught me and loved me. To them I dedicate this thesis.

Abstract

This work primarily focuses on the archetypal fullerene, which is C_{60} . C_{60} is electron rich, and yet can be six-fold reduced, taking on up to six additional electrons. Interest in the electrical properties of the solid state C_{60} were intensified when it was observed that it could be chemically doped with alkali metals, producing a metallic state A_1C_{60} , and even a superconducting state A_3C_{60} , where A indicates an alkali metal such as potassium or rubidium. Previous work has demonstrated that such a conductive state can also be achieved by optical pumping or by electron injection. The electronic properties of Fullerene films have, however, been shown to be highly dependent on film morphology. In a molecular solid, conductance in a perfect crystal is determined by intermolecular electron hopping, but in a polycrystalline film it is determined by interdomain hopping.

In this study thin films of fullerenes were sublimated on indium tin oxide coated glass substrates. The transparent indium tin oxide electrode allowed for in situ spectroscopic characterisation of the films while a thin aluminium top electrode completed the sandwich geometry for electrical characterisation. The thickness and optical absorption spectra of the deposited films were examined as a function of deposition time and deposition rate. Deposition rates were varied by altering the surface area of the evaporation boat. At low deposition rates, the absorption spectral profile was found to vary considerably and was not well correlated with deposition time. The spectral variations are comparable to those observed in annealed fullerene thin films and thus it was concluded that use of the small area evaporation boats, resulting in a low deposition rate, resulted in an effective annealing of the material prior to evaporation. Progressive

increase of the surface area of the evaporation boat resulted in a progressive increase of the evaporation rate. The absorption spectral profile then becomes better defined and correlates well with the deposition rate.

Current-Voltage (IV) measurements were carried out on a variety of films ranging in thickness from 100 nm to 800 nm, from each of the different boats. The IV characteristics showed that as the area of the boat increased the conductivity of the films decreased. The smaller boat area produced highly conductive films consistent with reported higher conductivities for annealed films. On the other hand the larger boat area produced lower conductivity films consistent with pristine C₆₀ films.

The temperature dependence of the conductivity, conducted under vacuum, indicated that at high deposition rates, the transport is a thermally activated hopping process, typical of molecular solids and therefore pristine C₆₀ films. Activation energies of between 0.3 eV to 1.1 eV have previously been reported for polycrystalline fullerene films. Analysis of the temperature dependence indicates a better fit to a variable range hopping process, however, indicative of amorphous films. In the films produced by low deposition rates, the conductivity is less temperature dependent, consistent with the behaviour of annealed fullerene films. The conductivities of the films produced by varying the deposition range from $1.8 \times 10^{-6} \text{ S cm}^{-1}$ to $7.1 \times 10^{-8} \text{ S cm}^{-1}$, the higher deposition rates producing lower conductivities. Although the higher conductivities may be attractive for some applications, the lower conductivities are more typical of pristine fullerene films.

It is concluded that the electronic and optical properties of fullerene films are highly sensitive to deposition parameters. The ability to produce polycrystalline films of well-defined physical characteristics requires precise control of many conditions and the variability of film morphology may be the root of the variability of reported electronic properties of fullerenes.

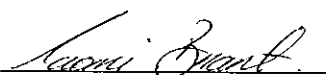
Declaration

I certify that this thesis which I now submit for examination for the award of M.Phil. is entirely my own work and has not been taken from the work of others save and to the extent that such work has been cited and acknowledged within the text of my work.

This thesis was prepared according to the regulations for postgraduate study by research of the Dublin Institute of Technology and has not been submitted in whole or in part for an award in any other Institute or University.

The work reported on in this thesis conforms to the principles and requirements of the Institute's guidelines for ethics in research.

The Institute has permission to keep, to lend or to copy this thesis in whole or in part, on condition that any such use of the material of the thesis be duly acknowledged.

Signature 

Naomi Brant

Contents

Chapter 1: Introduction	Page
1.1: General Introduction	4
1.2: Introduction to carbon	5
1.3: Bonding of carbon	6
1.4: Introduction to fullerenes	8
1.5: Conductivity and Superconductivity	10
1.6: Thesis Outline	14
Chapter 2: Structural and Theoretical background	
2.1: Fullerene Formation	19
2.2: Symmetry of C ₆₀	21
2.3: Electronic structure of C ₆₀	22
2.4: Solid state structure of C ₆₀	28
2.5: Summary	33
Chapter 3: Sample preparation and Experimental	
3.1: Film production	37
3.2: Thickness determination	39
3.3: Dektak ³ Method	41
3.4: Spectroscopic characterisation	42
3.5: Electronic Characterisation	46
3.6: Testing of films	48

3.7: Summary	50
Chapter 4: Spectroscopic Analysis	
4.1: Introduction	52
4.2: Film Analysis	52
4.3: Summary	60
Chapter 5: Electronic Analysis	
5.1: Transport properties in molecular materials	63
5.2: Variable range hopping	68
5.3 Current-Voltage Characteristics	69
5.4: Conduction Mechanisms	72
5.4.1: Richardson-Schottky emission	72
5.4.2: Poole-Frenkel effect	73
5.4.3: Space charge limited conduction	74
5.5: High voltage transport	75
5.5: Summary	78
Chapter 6: Conclusions	
Conclusions	81

Chapter 1

INTRODUCTION

1.1 General Introduction

Small structures with nanometre dimensions play a very important and ever growing role in biology, chemistry, physics, materials science [1] and everyday life. Examples are the large number of biomolecules which form the basis of life on earth and also small particles which act as catalysts for many chemical reactions [2]. In recent years, properties and structures of nano size materials have attracted the attention of numerous research groups. Their unique properties and small dimensionality indicate a very promising future for various potential applications.

Significant progress has been made towards understanding the properties and structures of nanometre scale materials and in this context well defined carbon molecular structures have played an important role. Since the discovery of carbon nano materials a large amount of theoretical and experimental work has been focused on the characterization of these materials [3]. C_{60} , discovered in 1985, was hailed as the third allotrope of carbon, after diamond and graphite, and dubbed buckminsterfullerene, because its molecular structure resembles the geodesic domes of futurist and architect Buckminster Fuller. The electrical, chemical, and mechanical properties of the material, often called buckyballs or fullerenes, led many scientists to imagine all sorts of potential uses: as semiconductor materials [2], for biomedical applications [4], and for building structures stronger than steel with a fraction of the weight of steel [5]. In the search for potential applications, much of the fundamental physics of molecular materials has been revisited and explored. In terms of potential applications and fundamental physics perhaps the most interesting is based on the electrical properties of fullerene solids, which have been shown to be insulating, metallic or even semiconducting [6,7]. As molecular solids, they are however soft materials and their structure, morphology and therefore physical properties can be

rather variable. This thesis outlines a systematic study of the dependence of the optical and electronic properties of fullerene thin films on preparation conditions.

1.2 Introduction to carbon

Carbon, an element of prehistoric discovery, is widely distributed in nature [8]. It is found in abundance in the sun, stars, comets and atmospheres of most planets. Carbon is the sixth most abundant element in the known universe but not nearly as common on the earth, despite the fact that living organisms contain significant amounts of the element. Common carbon compounds in the environment include the gases carbon dioxide (CO_2) and methane (CH_4). Pure carbon exists in several forms called allotropes as shown in Figure 1.1 below. Diamond is one form with a very strong crystal lattice; graphite is another allotrope in which the carbon atoms are arranged in planes, which are loosely bound to each other. The closed cage carbon molecular structures of fullerenes and nanotubes are commonly termed the third allotrope of carbon. In order to understand the origin of the range of differing forms it is important to understand the unique bonding configurations of carbon.

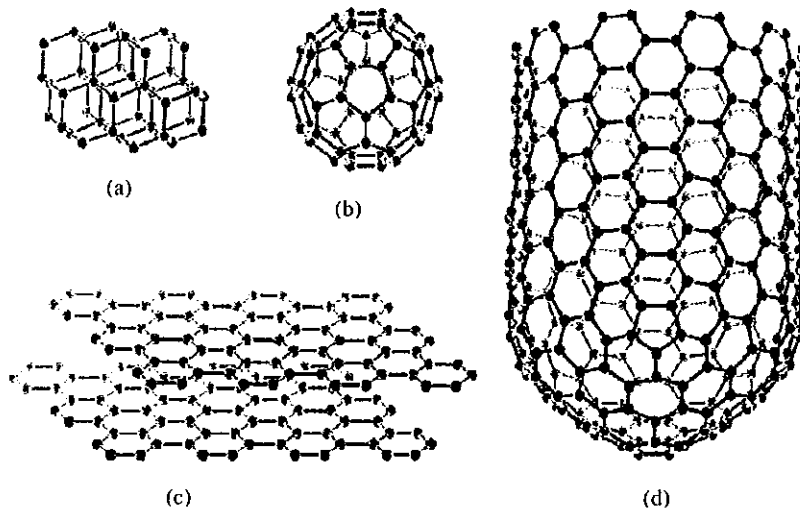


Figure 1.1: Various forms of carbon (a) Diamond, (b) Fullerene,
(c) Graphite and (d) Nanotube [9]

1.3 Bonding of carbon

Between atoms, the outer shell electrons can interact with each other to form chemical bonds resulting in molecules and solids. The exact nature of this bonding interaction depends largely on the electro negativities of the individual atoms. Bonds between atoms with large differences in electronegativity tend to be ionic, whereby electrons are fully donated from one atom to another. Bonds between atoms with identical, or slightly different electronegativity tend to be covalent, whereby the electrons are shared between the two atomic centers. Ionic and covalent bonds represent the limits of bonding, and covalent bonds between atoms with differing electro negativities will tend to be polarised, with the greatest electron density being associated with the most electronegative atom; again, ionic bonds represent the upper limit of this polarisation.

The electronegativity of an atom is governed by its tendency towards a closed shell configuration [10]. The orbital description of carbon being $1s^2 2s^2 2p^2$, would suggest a tendency to share or donate the outer two p electrons. However, carbon is known to coordinate in a four-fold fashion and in order to form four bonds, a 2s electron must be promoted to a p-orbital. The electronic configuration of carbon in such a state is $1s^2 2s^1 2p^3$ or more specifically $2s^1 2p_x^1 2p_y^1 2p_z^1$. The configuration can undergo a process known as hybridisation to achieve four valence electrons. Hybridization is the name used to describe the process of change from s and p atomic orbitals to sp bonding orbitals. The orbitals that have been changed are referred to as hybrid orbitals.

sp^3 hybridization involves the combination of the four atomic orbitals to form four identical tetrahedrally coordinated sp orbitals, each having one electron. Each sp orbital can form a strong (σ) bonding overlap with an orbital of a nearby atom producing for example CH_4 (methane). Such a bonding configuration is also responsible for the structure of diamond. The lattice is fourfold co-ordinated and all valence electrons are bound producing a rigid, transparent material. In the case where only two of the occupied p orbitals hybridise, an sp^2 configuration results. The three identical hybrid orbitals form strong σ bonds with nearby atoms. The remaining unhybridised p-orbital is orthogonal to the σ bonding plane and can form a weak π overlap with the p-orbital of a neighbouring carbon atom. Such a bonding configuration is present in C_2H_4 (ethane). The allotrope graphite is another example of sp^2 hybridised carbon. The plane of σ bonds forms the 2-D graphene sheets, in which the weakly bound π electrons are relatively free to migrate through the lattice. This electron delocalisation gives rise to metallic-like electronic properties and the black colour. Weak van der Waals bonding between graphene sheets results in graphite whereby the ability of the sheets to glide over each other produces

lubricant qualities. C_{60} is a further example of sp^2 hybridisation. The σ bonded sp^2 orbitals are responsible for the characteristic structure, whereas the weakly bound π electrons are the origin of its electronic and optical properties.

1.4 Introduction to fullerenes

Fullerenes were initially discovered in 1985 by a group of scientists, Harold Kroto, James Heath, Sean O'Brien, Robert Curl and Richard Smalley [3]. This group were actually trying to understand the absorption spectra of interstellar dust, which they suspected to be related to some kind of long-chained carbon molecules. While performing experiments they stumbled upon a strange material that had a peak at 720 amu in its mass spectrum. The amount synthesized was so little that structural analysis was virtually impossible but they hypothesized that 60 carbon atoms had formed themselves into a spherical arrangement. It was then proposed that a remarkably stable carbon cluster consisting of 60 carbon atoms was formed ($12\text{amu} \times 60 = 720\text{amu}$). The molecule, Figure 1.2, dubbed C_{60} , was named after the American architect R. Buckminster Fuller, who designed a geodesic dome with the same fundamental symmetry as that of the C_{60} molecule.

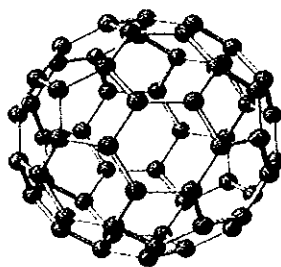


Figure 1.2: Structure of the C_{60} molecule showing soccer ball shape

Furthermore, it turned out that C_{60} was only the first of an entire class of closed cage molecules consisting of only carbon atoms. This new family of molecules were collectively known as fullerenes (C_{60} , C_{70} , C_{82} , C_{120} ..etc) [3]. Their discovery attracted the attention of researchers worldwide.

Initially, when C_{60} was first discovered it could only be produced in very small quantities. As a result there were only a few kinds of experiments that could be performed on the material. In 1990, five years after its discovery, everything changed dramatically when Wolfgang Krätschmer, Lowell Lamb, Konstantinos Fostiropoulos, and Donald Huffman discovered a method of producing pure C_{60} in much larger quantities [11]. Their design involved resistive heating of graphite in an arc discharge chamber to generate these macroscopic quantities of fullerenes. This opened up completely new possibilities for experimental investigations. The proposed structure was confirmed by Nuclear Magnetic Resonance (NMR) [12,13] and a period of very intensive research in the field was launched. Nowadays, it is relatively straightforward to mass-produce C_{60} and it is one of the most researched nanomaterials to date

There are many proposed applications for the buckyballs, ranging from rocket fuel [14,15] to anti-AIDS medicine [16]. The pharmaceutical industry is exploiting its inert state and its ability to bond with an, as yet, indeterminate number of other elements, molecules and chains. It is in use in AIDS research and chemotherapy and is hoped to serve as a delivery vehicle for chemical treatments [16]. For example C_{60} is just the right size to fit into the active cavity of HIV Protease, an enzyme important to the activity of the virus which causes AIDS. Cramming a buckyball into the active cavity would deactivate the enzyme and kill the virus. Methods for getting the molecule to the

enzyme are under investigation [4,16]. The size of the C₆₀ molecule is similar to many active biological molecules; this gives it potential as a foundation for creating a variety of biologically active variants [5,16].

When compressed, fullerenes can become twice as hard as diamond and can therefore be used as a very accurate cutting tool for steel and other hard materials [17]. Physically, buckyballs are extremely strong molecules that are able to withstand high pressures [5]. However, in their pristine form they do not bond to each other chemically, sticking together through weak van der Waals forces. This is the same force that holds layers of graphite together, which would also give buckyballs the potential as a lubricant. Use of fullerenes in optical devices have been studied [18].

Thermal instability, ability to form clusters and sparing solubility of fullerenes has imposed limitations on the direct use of these materials, however. In contrast, when doped within other host materials, such as silica, polymers or metal clusters, they gain practical value. The optical limiting behavior of these materials is observed through typically measurements using ultraviolet/visible (UV/Vis) spectroscopy and photoluminescence [18]. The high damage threshold makes it possible to use such hybrids in laser applications.

1.5 Conductivity and Superconductivity

Pure C₆₀ is known to be a molecular insulator but it can change its properties in the crystalline solid state, from insulating to conducting or even superconducting, as a result of numerous factors. Fullerenes are very large graphitic systems and can therefore

easily accommodate extra electrons. Voltametric measurements of C_{60} in solution have shown that the molecule can stably accept up to 6 electrons [19]. In the hexagonally close packed crystalline solid state, electron donating dopants can thus generate lattices of negatively charged fullerenes. A metallic state can be achieved by doping the lattice with one alkali atom per molecule of C_{60} to produce A_1C_{60} [20]. In this stoichiometry the fullerene lattice is made up of singly charged fullerene molecules. When three electrons are added to C_{60} in the form of A_3C_{60} a superconducting state can be achieved. These hybrid materials are actually pseudo metallic, and display superconductivity at low temperatures ($T_c=45$ K) [21]. It has been shown that A can be any metal in Group I (lithium, sodium, potassium, rubidium, cesium) producing superconducting transition temperatures in the range 10-40 K, depending which alkali metal is used. These salts show characteristic signs of superconductors, in that there is an expulsion of magnetic flux at low temperatures and zero resistance to electrical current [22]. Current research is aimed at getting the maximum superconducting transition temperature (or T_c) to higher values. This insulator to metal-like transition has also been achieved by optically pumping single crystals of fullerenes with a laser [23]. Unlike chemical doping this process is fully reversible, once the laser is turned off the flow of electrons is stopped and so the film can be switched between insulating to metallic characteristics. However this can be costly due to the fact that very high-powered lasers are required to achieve this transition.

Electrically induced transitions from insulator to metal-like in single crystals and also thin films of C_{60} have also been demonstrated [22,24]. Figure 1.3 shows a typical current-voltage characteristic of pristine C_{60} thin film at 20K. Previous reports on the conductivity of C_{60} films at low temperatures have shown that increasing the voltage

results in an increase in the current of several orders of magnitude [25]. This dramatic “jump” in conductivity happens at a critical current density when an electron path is produced through the material and so making it easier for the following electrons to get through. It is noticed that as the voltage is reduced the new current-voltage (IV) curve follows the initial curve until a certain point. At this point it does not revert to its initial low conductance state but is seen to decrease linearly. A further reduction in voltage results in an abrupt switch back to low currents. This process has been shown to be completely cycleable, as in the film can be switched back and forth from the low to high conduction states. Also the highly conductive state is stable for long periods and the curve is reproducible.

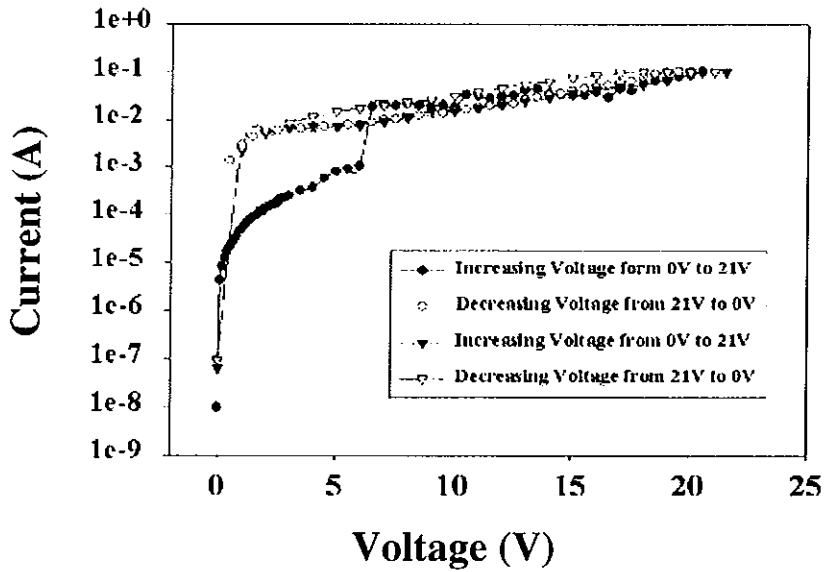


Figure 1.3: IV characteristic of ITO/C₆₀/Al thin film at 20K [26]

The ability to reversibly switch from insulating to metallic (and potentially superconducting) behaviour by application of relatively low voltages is attractive for a range of potential applications. However, both optically and electronically the effect is

not well characterised and can vary substantially from sample to sample. There is a strong indication that the effect is dependent on crystallite size and quality [27].

Both optical and electronic processes in fullerenes have also been shown to be strongly temperature dependent. Figure 1.4 demonstrates the IV characteristics of the same sample as Figure 1.3 at room temperature. A similar dramatic increase in conductivity is observed, but a rapid decrease is subsequently observed upon a further increase in voltage. Beyond a certain voltage the characteristics were seen to be irreversible, thus indicating a structural change in the material. It has been previously reported by Smie and Heinze that the presence of the second maxima can be attributed to the formation of dimeric dianions [28]. This suggests that the C_{60} lattice may be unstable to the addition of electrons and is subject to collapse.

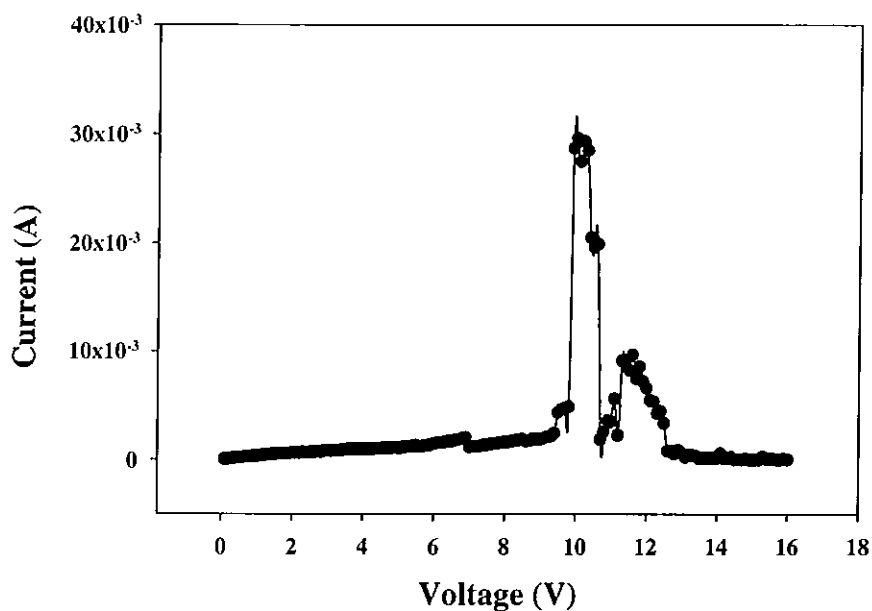


Figure 1.4: IV characteristics observed for Pristine ITO/ C_{60} /Al structure at 300K [26]

Chemically, fullerenes are quite stable; breaking the balls requires temperatures of over 1000°C [13]. At much lower temperatures (a few hundred degrees C) fullerenes will "sublime," which means vapour will form directly from the solid. The balls don't break; they just separate from the solid intact. However, the van der Waals solid-state lattice is soft and has been shown to polymerise at room temperature under prolonged illumination [29]. Hydrostatic pressure has been shown to result in a similar polymerisation [30]. The strong temperature dependence of such phenomena is related to the phase transition in the lattice whereby the rotational freedom of the molecules at room temperature is frozen out below ~249K [31].

The low voltage transport processes of fullerene solids are also strongly affected by this rotational phase transition [32]. As a molecular solid, transport relies on intermolecular hopping, a processes which is enhanced by rotational freedom [33]. Exposure to oxygen has been shown to have a detrimental effect on both the dark and photoconductive behaviour [34] of fullerenes. Thermal annealing has been shown to induce a transition from a thermally activated transport mechanism to a more metallic-like temperature independent behaviour [34].

1.6 Thesis outline

Although C₆₀ appears an attractively simple molecule, which orders into apparently textbook crystalline structures, its physical properties can be extremely complex. Fascinating electronic transitions from insulating to metallic and superconducting can be produced by doping, but the phenomena are strongly dependent on sample preparation and external factors such as temperature and oxygen contamination. In

many cases, the ideal behaviour is observable in single crystals of some 100's of micron dimensions, which are difficult to handle, but reproducible results are not observable in polycrystalline films. This thesis outlines a study to examine the dependence of the optical and electronic properties of vacuum sublimed fullerene thin films on deposition parameters.

Chapter 2 shows the fullerene formation model and how they are produced. Also the symmetry of C_{60} is introduced. This chapter also shows the electronic structure of the isolated molecule in comparison to the solid-state structure. Chapter 3 explains the experimental methods starting with the production of the films themselves. Then there is the thickness determination and how measurements were conducted. Spectroscopic characterisation is also presented in this chapter along with the characterisation of the set up. A description of how the films were tested, by the use of electron injection, is also given in this chapter. In Chapter 4 the effect of the boat area on the films is studied. The absorption spectra are seen to become more reproducible the larger the boat area. Chapter 5 discusses transport properties in molecular solids. This chapter also shows the current-voltage characteristics obtained from each of the different boats used and some of the conduction mechanisms involved in the thin films are explained. It can be seen that boat area is an important parameter in the production of pristine fullerene films. The final chapter is a discussion of the results obtained and the conclusions that can be deduced from these results.

References

1. M. Rieth, "Nano-Engineering in Science and Technology – An Introduction to the world of nano-design", *World Scientific* (2003)
2. A. Goel and J. Howard, *Carbon* 41, 1949 (2003)

3. H. Kroto, J. Heath, S. O'Brien, R. Curl, and R. Smalley, *Nature* 318, 162-163 (1985).
4. S. Freidman, D. DeCamp, R. Sijbesma, G. Srdanov, F. Wudl, and G. Kenyon, *J.Am.Chem.Soc.*, 115, 6506-6509 (1993).
5. P. Holster, C. Román, T. Harper, *Cientifica* (2003)
6. M. Golden, M. Knupfer, J.Fink, J. Armbruster, T. Cummins, H. Romberg, M. Roth, M. Sing, M. Schmidt, E. Sohmen, *J. Phys: Condens. Matter* 7, 8219 (1995)
7. J. Weaver, D. Poirier, in: H. Ehrenreich, F. Saepan (Eds), *Solid State Physics*, 48, p.1, Academic press, New York (1994)
8. N. Pace, *Proceedings of the National Academy of Science*, 98, 805 (2001)
9. www.cnanotech.com/pages/resources_and_news/gallery/ (April 2005)
10. J. Xu and Y. Jiang, *j. Chem. Inf. Comput. Sci*, 35, 214-216 (1995)
11. W. Krätschmer, L. D. Lamb, K. Fostiropoulos, D. R. Huffman, *Nature* 347, 354, (1990).
12. W. Krätschmer, K. Fostiropoulos and D.R. Huffman *Chem. Phys. Lett.* 170, 167, (1990).
13. H. Ajie, M. A. Marcos, J.A. Samir, B.D. Rainer, and W. Krätschmer, *J. Phys. Chem.* 94, 8630, (1990).
14. H. Aldersey-Williams "The most Beautiful Molecule" John Wiley and sons Inc (1995).
15. J Baggott, "Perfect Symmetry" Oxford Press (1996).
16. T. Pradeep, *Current Science*, 72, 124, (1997)
17. A. Gion, *Bucky Balls*, <http://www.3rd1000.com/bucky/bucky.htm>, (Nov 2005)
18. L.W. Tutt and A. Kost, *Nature* 356, 225 (1992)
19. T. Tatsuma, S. Kikuyama, and N. Oyama, *J. Phys. Chem*, 97, 12067 (1993)

20. M. Dresselhuas, G. Dresselhaus, P. Eklund, *Science of Fullerenes and Nanotubes*, Academic press, New York (1996)
21. A. Hebard, M. Rosseinsky, R. Haddon, D. Murphy, S. Glarum, T. Palstra, A. Ramirez and A. Kortan, *Nature* 350, 600 (1991)
22. H. Weber *App.Phys Lett.* 81, 3749, (1998)
23. S. Brorson, M. Kelly, U. Wenschuh, R. Buhleier and J. Kuhl, *Phys. Rev. B* 46, 7329 (1992)
24. J. G. Simmons, *Phys. Rev.*, 155, 657 (1967)
25. G. Chambers and H. Byrne *Mol. Mater.* 13, 193-200 (2000)
26. S. Phelan, MPhil dissertation, Dublin Institute of Technology (2004)
27. H. Byrne, W. Maser, W. Rühle, A. Mittelbach and S. Roth, *Appl. Phys. A*, 56, 235 (1992)
28. A. Smie and J. Heizne, *Physics and Chemistry of Fullerenes and Derivatives*, World Scientific Singapore (1995)
29. L. Akselrod and H. Byrne *Chem. Phys. Lett.* 215, 131 (1993)
30. H. Yamawaki, M. Yoshida, Y. Kakudate, S. Usuba, H. Yokoi, S. Fujiwara, K. Aoki, R. Ruoff, R. Malhotra, and D. Lorents, *J. Phys. Chem.* 97, 11161 (1993)
31. H. Kuzmany, M. Matus, B. Burger, *J. Winter, Adv. Mater.* 10, 731 (1994)
32. P. van Loosdrecht, P. van Bentum, M. Verheijen and G. Meijer, *Chem. Phys. Lett.*, 198, 587 (1992)
33. M. Paulsson and S. Stafström, *J. Phys.: Condens. Matter* 12, 9433 (2000)
34. M. Kaiser, W.K. Maser, H.J. Byrne, A. Mittelbach and S. Roth, *Solid State Commun.*, 87, 281 (1993)

Chapter 2

STRUCTURAL AND THEORETICAL BACKGROUND
OF FULLERENES

2.1 Fullerene Formation

Fullerenes are molecules that are made up of 60 carbon atoms arranged in a series of interlocking hexagons and pentagons, forming a structure that looks similar to a soccer ball [1]. C_{60} is actually a "truncated icosahedron", consisting of 12 pentagons and 20 hexagons. For each fullerene with only pentagonal and hexagonal faces there must be 12 pentagons and an arbitrary number of hexagons. Euler's law for closed shell polyhedra, which can be shown mathematically, arrives at this minimal number of pentagons.

$$v+f = e+2 \quad \text{Equation 2.1}$$

where v is the number of vertices, f is the number of faces, and e is the number of edges in the polyhedron. In fullerenes only pentagons and hexagons are considered, so for p pentagons and h hexagons the number of faces should equal:

$$f = p+h \quad \text{Equation 2.2.}$$

Among general fullerenes the class consisting of 5/6 fullerenes with pentagonal and hexagonal faces can be distinguished. If n_5 is the number of pentagons and n_6 is the number of hexagons then the equations will result in $p = 12$ as shown. The number of bonds in this molecule will be equal to the number of edges (e) and since each edge joins two faces:

$$2e = 5p+6h \quad \text{Equation 2.3}$$

The number of edges is equal to $3v/2$, so therefore:

$$3v = 5p + 6h \quad \text{Equation 2.4}$$

$$e = (5p + 6h) / 2 = 3v / 2 \quad \text{Equation 2.5.}$$

These equations lead to:

$$6(f + v - e) = p = 12 \quad \text{Equation 2.6.}$$

Hence the smallest fullerene is C_{20} , built up of 12 pentagons and no hexagons. However when two pentagons are adjacent to each other, there is a high local curvature and so, a high strain in these carbon structures. There is an “isolated pentagon rule” which states that the stable, non-reactive fullerene is only formed when the pentagons at the surface are separated. C_{60} is the smallest fullerene that obeys this isolated pentagon rule [2] the next is C_{70} .

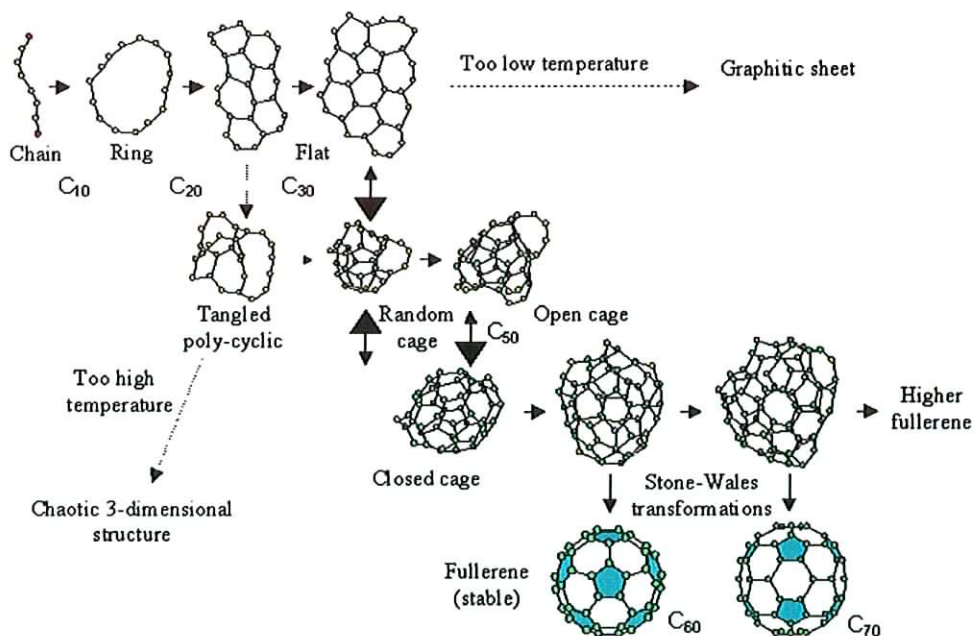


Figure 2.1: Proposed fullerene formation model. [3]

2.2 Symmetry of C_{60}

The most striking property of the C_{60} molecule is its high symmetry. This means many transformations that map the molecule onto itself can be found. All of these symmetry operations for a molecule are rotations around an axis, reflections in a plane, and also sometimes inversions. The symmetry operations must leave the centre of mass of the molecule in place, so all rotation axes and mirror planes must go through that point. For the C_{60} molecule there are three kinds of rotation axes. The most obvious ones are the 5-fold axes through the centres of two facing pentagons. Look down on one of the pentagons and you see that the molecule is symmetric under rotations of $360/5 = 72$ degrees. Next there are rotation axes through the centre of two facing hexagons. Observe that these axes are only 3-fold, i.e. it takes a rotation of 120 degrees to map the molecule onto itself. Finally there are 2-fold axes through the centres of the edges between two hexagons. Since there are 12 pentagons, there are 6 different 5-fold axes, each axis passes through two pentagons. Likewise, since there are 20 hexagons, there are 10 different threefold axes. To find the number of different two-fold axes, each hexagon is neighboured by three other hexagons. Hence there are 30 edges between two hexagons, i.e. 15 different 2-fold axes. The reflection symmetries are also related to the edges between adjacent hexagons. The mirror planes contain two such edges hence there are also 15 different mirror planes. Finally, the C_{60} molecule is invariant under the inversion with respect to the centre of mass. This means that if you replace each point with coordinates (x,y,z) by $(-x,-y,-z)$, the molecule is mapped onto itself. Combining all those transformations, one finds 120 different symmetry operations. They form the icosahedral group, which is the point group with the largest number of elements. Hence C_{60} can be called the most symmetric molecule. The C_{60} molecule is a regular truncated

icosahedron, with a point group I_h , the symmetry operations of which consists of the identity operation, 12 five-fold axes through the centre of the pentagonal faces, 20 three-fold axes through the centres of the hexagonal faces, 15 two-fold axes through centres of the edges joining two hexagons. Each of the 60 rotational symmetry operations can be compounded with the inversion operation, resulting in 120 symmetry operations in the icosahedral point group I_h . Figure 2.3, shows the rotational symmetries of the C_{60} molecule.

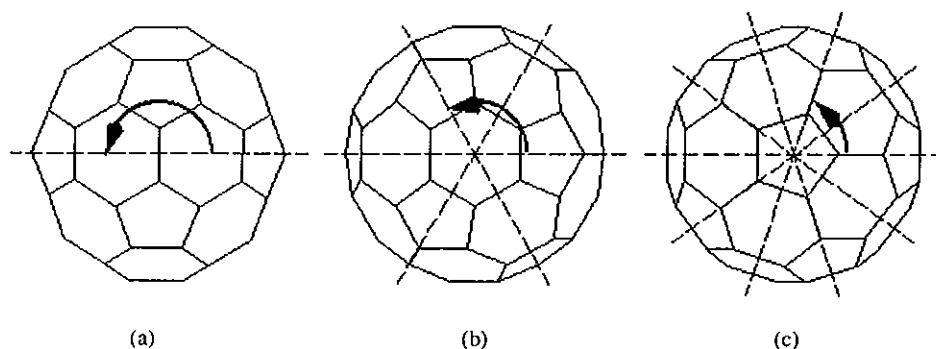


Figure 2.2. Rotational symmetries of the C_{60} molecule. (a) Twofold axes pass through opposing pairs of hexagon-hexagon edges, (b) threefold axes connect midpoints of hexagonal faces related by inversion, (c) fivefold axes connect midpoints of the pentagonal faces related by inversion [4].

2.3 Electronic structure of the C_{60} molecule

To fully understand the electronic properties of solids, it is useful to take a look at the electronic structure of an isolated C_{60} molecule first. The simplest possible approach to this is based on the Hückel molecular orbital calculations of Haddon [5]. C_{60} has 240 valence electrons, but each carbon atom has three σ (sigma) bonds to its neighbours,

using up a total of 180 electrons for this purpose. The energy of these electrons is well below the Fermi surface. They stabilize the structure, but do not contribute to the conduction. The remaining 60 electrons are distributed around the molecule on orbitals that originate from the (much less tight) carbon–carbon π orbitals. These orbitals are somewhat similar to the π electron orbits of a graphene plane, with two important differences. First, the three bonds around a carbon atom in C_{60} (or in any other fullerene) do not make a plane, whereas in graphene the electrons have equal probability of being ‘below’ and ‘above’ the plane. In fullerenes the π electrons tend to spend more time outside of the ball than inside. Second, in C_{60} the C–C bond lengths are not uniform; the π electrons are not truly ‘delocalized’ around the six-member carbon rings (like in benzene or graphene), but they are distributed over 30 ‘bulges’ of electronic orbits that stick out of the C_{60} molecule. A somewhat lower electron density belongs to the other 60 orbitals connecting the carbon pairs with longer bond lengths. The overlap between these orbitals on adjacent molecules will determine the properties of the conduction electron band of the doped solids. A first insight into the nature of the molecular orbitals can be obtained by borrowing ideas from the early days of nuclear physics, when the quantum mechanics of particles confined in a spherical potential well was first considered. In this case the states are still labeled by quantum numbers n , l and m , but the peculiar degeneracy of the different angular momentum states, that characterizes the textbook treatment of the hydrogen atom, does not apply. In a steep-walled potential well (like a nucleus or a C_{60} molecule) the lower l states will have lower energy. Consider 60 non-interacting electrons, confined to a sphere on a high- n orbit with various l . The first two electrons will fill the $l = 0$ state. Proceeding to higher l , one has to count the number of available states, $N = 2(2l + 1)$ (where the first factor of 2 stands for spin). It is easy to see that, on reaching $l = 4$, altogether 50 electrons are consumed. The remaining ten

electrons will all go to the $l = 5$ state. Hückel molecular orbital calculations find that the simple picture described above works well for $l = 0, 1, 2, 3, 4$, but for higher energies the 'spherical potential' approximation is no longer useful. In order to go any further energy splitting due to the true atomic potentials needs to be looked at. In the real C_{60} , l is not a good quantum number, and the electronic orbitals should be labeled according to the irreducible representations of the icosahedral symmetry group. The orbitals available for the remaining ten electrons are, in order of increasing energy, the h_u , the t_{1u} and the t_{1g} levels [5]. The degeneracy of these levels (including spin) is 10, 6 and 6 respectively. The h_u level is completely filled by the ten remaining electrons, becoming the highest occupied molecular orbit (HOMO), and the t_{1u} level becomes the lowest unoccupied molecular orbit (LUMO). The HOMO-LUMO gap is roughly 1.9 eV. In the spherical approximation the HOMO and the LUMO bands all belong to $l = 5$, and the corresponding Hückel molecular wave functions carry some of the $l = 5$ character [5]. The remaining six states in the $l = 5$ representation are pushed to such a high energy that the six fold degenerate t_{1g} orbitals follow the LUMO band. This level, with an $l = 6$ character, becomes the LUMO + 1 level. In the solid state the bands originating from the HOMO and LUMO levels are the most important ones, as they are in the immediate vicinity of the Fermi surface. The crystal fields reduce the molecular symmetry and the energy levels split. The overlap of orbitals broadens the levels to bands. In the simplest possible cubic environment a few of the molecular levels preserve their symmetry and survive without splitting. The relative orientation of the molecules has a strong influence on the overlap of molecular orbitals [6]. In a realistic model the unit cell must include more than one molecule and the calculation becomes increasingly complex [6]. In a few important cases there is a residual randomness (e.g., the merohedral disorder) to the structure. The translational invariance, suggested by the molecular centers, is broken by

the orientational disorder. Strictly speaking, the electronic wave number is not a good quantum number, and the band structure is not a good concept. Yet the metallic behaviour cannot be excluded: just as in amorphous metals, the electrons can still propagate in the lattice, except that the propagation is diffusive rather than ballistic. The density of states can be calculated and a bandwidth of about 0.5 eV is obtained for the LUMO band [7-10].

The electronic ground state of C_{60} is a closed shell and has A_g symmetry. The five lowest excited configurations and the corresponding state symmetries are:

HOMO	→ LUMO	$h_u \rightarrow t_{1u}$	T_{1g}, T_{2g}, G_g, H_g
HOMO - 1	→ LUMO	$h_g \rightarrow t_{1u}$	T_{1u}, T_{2u}, G_u, H_u
HOMO	→ LUMO + 1	$h_u \rightarrow t_{1g}$	T_{1u}, T_{2u}, G_u, H_u
HOMO - 1	→ LUMO + 1	$h_g \rightarrow t_{1g}$	T_{1g}, T_{2g}, G_g, H_g
HOMO - 2	→ LUMO	$g_g \rightarrow t_{1u}$	T_{2u}, G_u, H_u

These can be seen in Figure 2.3, which shows both the atomic orbital model and the Hückel molecular orbital model.

Electronic Structure of C₆₀

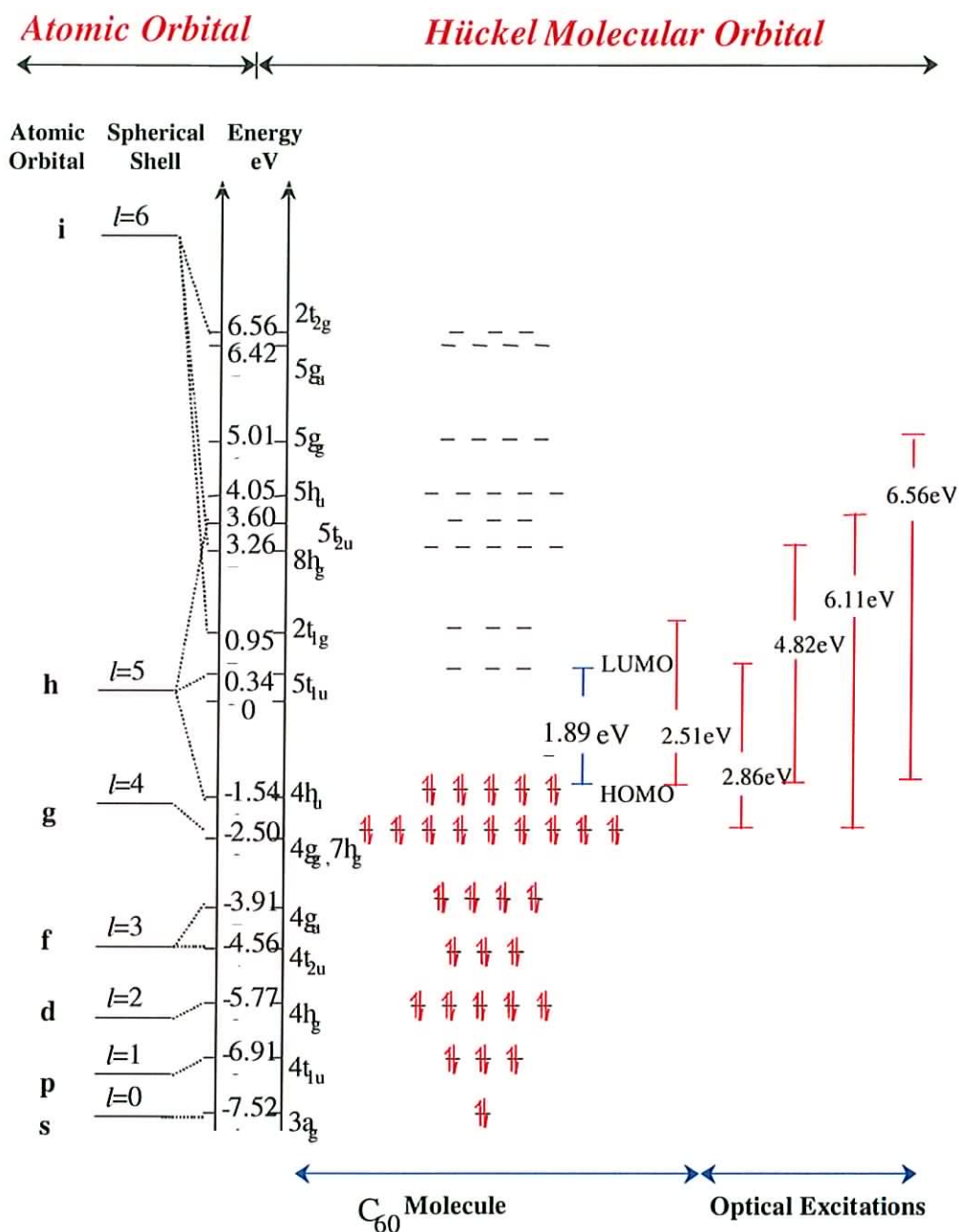


Figure 2.3: Electronic structure of the C₆₀ molecule showing the molecular orbits [11]

As mentioned above, the states deriving from the lowest excitation from the HOMO to the LUMO, i.e. h_u to t_{1u} , give an energy gap value of ~ 1.9 eV for C_{60} molecules in solution. The electric dipole moment transition between the A_g ground state and an excited state is allowed only for T_{1u} excited states. Transitions from the ground state to states of other symmetries are forbidden and can occur only by means of the activity of suitable non-totally-symmetric vibrations, *via* the Herzberg - Teller vibronic coupling mechanism, which results from the mixing of the different vibrational states by vibrationally induced charge transfer in the electronic wave functions, or Jahn - Teller distortions, which describe the geometrical distortion of the electron cloud in a non-linear molecule under certain conditions. The excited states of lower energy, which originate from the HOMO-LUMO excitations, are symmetry forbidden and thus the absorption spectrum is expected to begin on the low energy side with very weak bands.

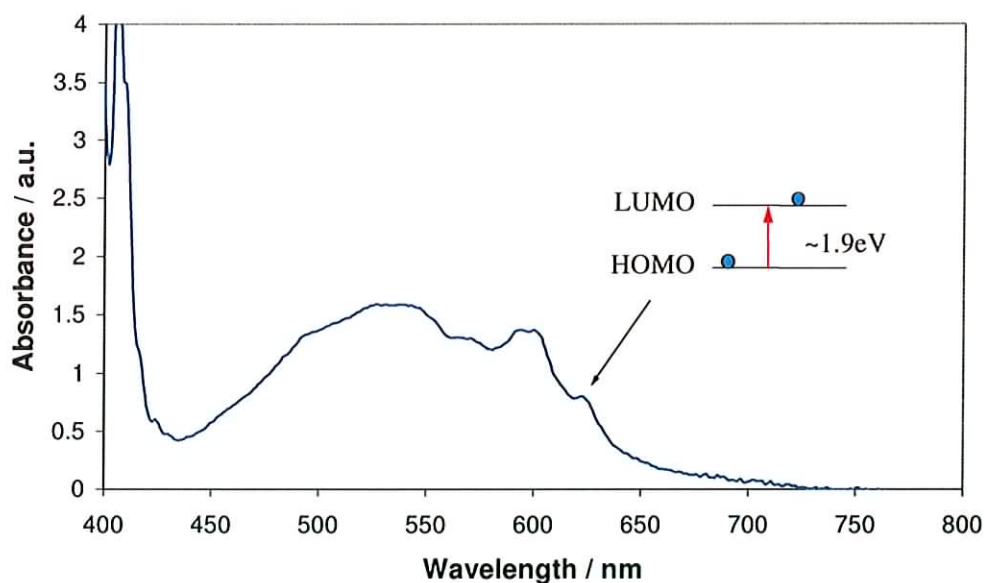


Figure 2.4: Absorbance spectra of C_{60} solution in chloroform (30mg/10ml)

Figure 2.4 shows a typical absorption spectrum for C_{60} in solution, with a concentration of 30mg/10ml. The solution was then placed into a cuvette and the spectrum was recorded between 400-800 nm using the UV/Vis spectrometer described in Chapter 3. In C_{60} the closed shell icosahedral symmetry renders the HOMO-LUMO, lowest energy, transition dipole forbidden. Nevertheless this HOMO-LUMO transition is visible in the absorption spectrum of C_{60} , as indicated above, around 620 nm. This transition gives C_{60} solutions their distinctive burgundy colour.

2.4 Solid State Structure of C_{60}

As well as looking at the molecular structure of C_{60} it is also important to look at how these molecules interact with each other when in the solid state. This involves observing the way in which the C_{60} molecules pack together and arrange themselves in the bulk solid. Previous reports have shown that at room temperature the centers of the C_{60} molecules make an fcc lattice, with a nearest-neighbour C_{60} - C_{60} distance that corresponds to the diameter of the molecule [12]. An fcc close-packed structure is constructed by placing close-packed layers on top of one another. The first layer consists of spheres in contact, with each sphere having six nearest neighbours in the plane. Placing spheres in the dips of the first layer forms the second layer. The spheres of the third layer are placed above the gaps in the first layer. Thus the second layer covers half the holes in the first layer and the third layer lies above the remaining holes. This arrangement results in an ABCABC ... pattern and corresponds to a lattice with a face-centered cubic unit cell (Figure 2.5). Spheres sit at the eight corners and at the centers of the six sides of the cubic unit cell, which has an edge length ("lattice constant") of a , which in C_{60} is 14.17 Å [12]. The distance between nearest neighbours (corner sphere to face sphere) is $(\sqrt{2}/2)a$,

giving a value of 10.02 Å for the C₆₀ molecule. Table 2.1 below shows a list of important physical constants for the C₆₀ molecule and solid state [13].

Table 2.1: Shows the physical constants for C₆₀ molecules and crystalline C₆₀ in the solid state

Quantity	Reference Value [13]
Average C-C distance	1.44 Å
C-C bond length on a pentagon	1.46 Å
C-C bond length between adjacent hexagon	1.40 Å
C ₆₀ mean ball diameter	7.10 Å
C ₆₀ diameter including electron cloud	10.34 Å
fcc Lattice constant	14.17 Å
C ₆₀ – C ₆₀ centre to centre distance	10.02 Å
C ₆₀ – C ₆₀ cohesive energy	1.6 eV

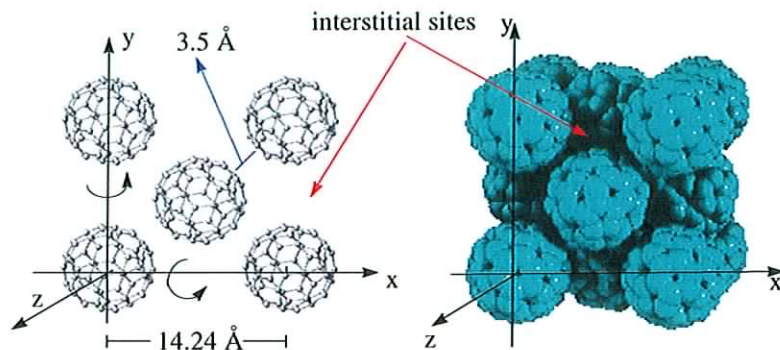


Figure 2.5: Solid State Structure of C_{60} [11]

If the electron cloud (Figure 2.6) of the molecule is taken into consideration then the nearest neighbour distance can be reduced to 3.5 Å. This can be achieved by the injection of electrons into the lattice. The electron clouds then become distorted and begin to overlap causing interactions to occur between the molecules.

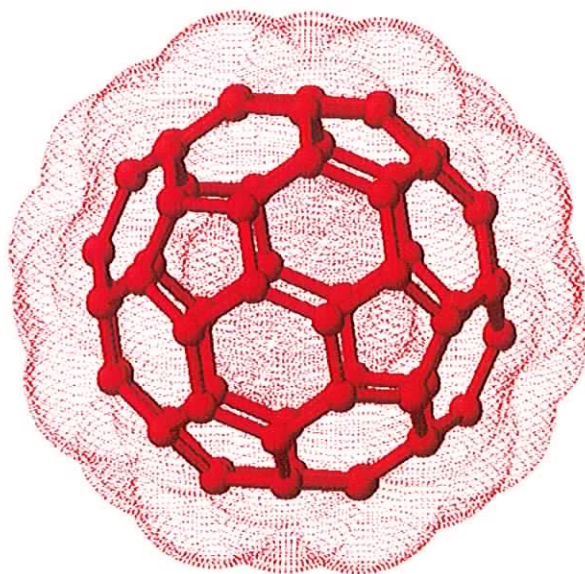


Figure 2.6: Shows the proposed truncated icosahedral structure of the Buckminsterfullerene (C_{60}) with its electron cloud. Note a popular representation of this structure is a football.[11]

At room temperature the molecules spin freely and independently of each other. This room temperature fcc phase is known as the rotary phase due to the rotation of the molecules. As the temperature is lowered, the rotation of the molecules stops. The centers of the molecules remain in the same place, but the incompatibility of the icosahedral molecular symmetry and the cubic lattice symmetry makes it impossible to describe the structure in terms of the simple fcc lattice (with one C_{60} molecule of fixed orientation each unit cell). However, it may be still possible to view the structure in terms of a larger unit cell, and a simple cubic lattice (Figure 2.7). The freezing of the rotational motion actually happens in two stages. First, at 249 K the rotational axis of each molecule becomes constrained. The building block of the new structure consists of four C_{60} molecules arranged at the vertices, with each one of them spinning around a different, but well defined axis. Then, at lower temperatures, the rotation around these axes slows and gradually stops. Below about 90K the molecules are entirely frozen, but they never order perfectly. In solid C_{60} there is always a ‘merohedral disorder’, due to the different molecular orientations [14].

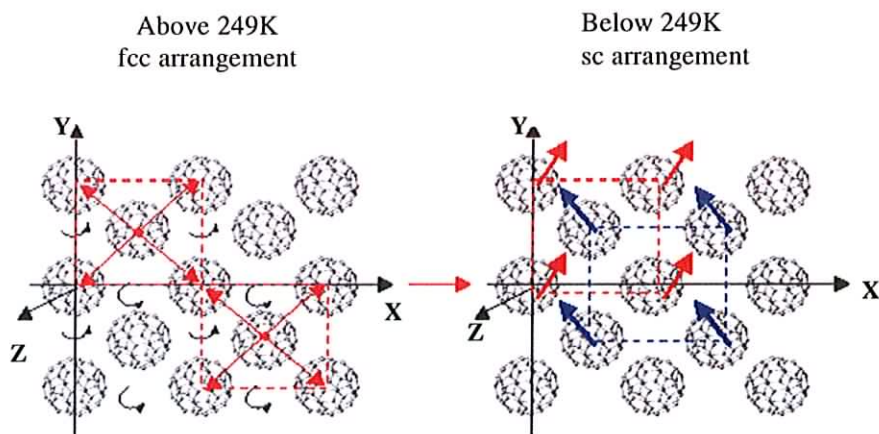


Figure 2.7: Above 249K, the molecules are rapidly spinning, giving rise to a fcc type lattice arrangement.

However below 249K the spinning motion is frozen out and a simple cubic type lattice results [15]

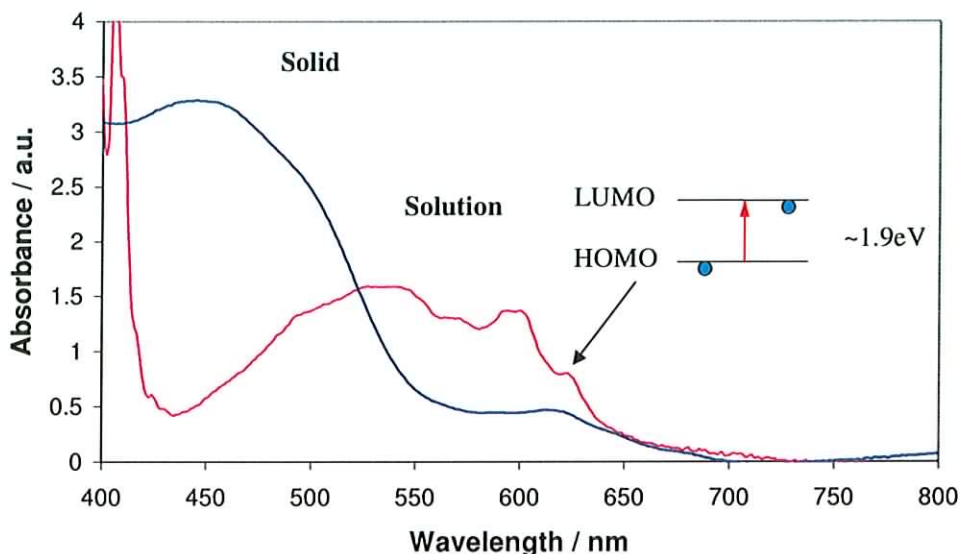


Figure 2.8: The absorption spectra in thin film and in solution form

Figure 2.8 shows a comparison of the absorption spectrum of C_{60} in solution (isolated molecule) and a solid C_{60} film. It can be seen that in the solid state the absorption spectrum is slightly red shifted from that of the isolated molecule [16]. This shows that the solid state of C_{60} appears to behave like a classical molecular solid. In comparing the spectra, it can be seen that the HOMO-LUMO transition is present in both (~ 620 nm, 1.9 eV), but there is an absorption at ~ 400 - 550 nm, which appears strongly in the solid-state spectrum but not in that of the isolated molecule. This feature is absent from the solution absorption spectrum, which suggests that it is not molecular in origin. It is the result of an intermolecular charge transfer excited state [17]. In the classification of solid-state band theory the optical excited state of C_{60} may be considered by Frenkel-like exciton states. The Frenkel exciton picture is valid if the exciton binding energy, which is the energy required to take an electron from a molecule and to put it on a

different molecule in the solid is much larger than the energy of exciton transfer between molecules. In solid C_{60} this condition is well satisfied. However when molecules form a solid state, intermolecular charge transfer (CT) excitations become possible in addition to Frenkel Excitons. A charge transfer excitation corresponds to a creation of an electron and the hole on different molecules. If an electron and a hole are situated on nearest neighbour molecules and are bound to each other, then they are called a CT exciton. However, this does not mean that they are localised on two molecules. In the fcc lattice of C_{60} , the electron can be located on any one of the twelve equivalent nearest neighbour molecules around the molecule occupied by the hole, and vice versa. A CT exciton exists once the electron and hole are separated by one or more lattice distances but are still correlated to each other. The absorption at ~ 450 nm is in fact composed of a double CT state, corresponding to the edge and diagonal nearest neighbour overlap, and the relative intensity of these two bands has been shown to be strongly dependent on morphology and can be altered through for example thermal annealing [18]. Furthermore, although the fullerene molecules themselves are highly stable, in the solid they are weakly bound and any perturbation causes a change to the equilibrium configuration and collapse of the system. It has been shown that the C_{60} lattice is unstable to the addition of electrons and is prone to polymerisation above ~ 249 K [19].

2.5 Summary

C_{60} is the third allotrope of carbon. These molecules are made up of 60 carbon atoms arranged in a series of interlocking hexagons and pentagons, forming a soccer ball like structure. In order to get a fully comprehensive understanding of the electronic

properties of solids it was necessary to take a look at the electronic structure of an isolated C₆₀ molecule. The h_u level is completely filled by the ten remaining electrons, becoming the highest occupied molecular orbit (HOMO), and the t_{1u} level becomes the lowest unoccupied molecular orbit (LUMO). The HOMO-LUMO gap is the lowest energy transition and is about 1.9 eV. Variations in the absorption spectra for the solid and solution were observed indicating an interaction between the molecules in the solid state. It is this degree of intermolecular interaction in the solid state, which is thought to contribute to conductivity. C₆₀ forms a molecular solid but although these molecules weakly interact, there is not a huge change to the electronic structure of the molecule. However, an additional excited state specific only to the solid has been identified. This state is proposed to be characteristic of intermolecular electronic interactions in the crystal lattice. At room temperature the molecules are free to rotate around their lattice positions in a face centered cubic configuration. At lower temperatures, below 249K [14], these rotations are frozen resulting in the lattice adopting a simple cubic arrangement. This change in lattice structure is expected to influence the electrical interactions of the molecules.

References

1. H.W. Kroto, J.R. Heath, S.C. O'Brien, R.F. Curl, and R.E. Smalley, *Nature* 318, 162-163 (1985).
2. H.W. Kroto, *Nature* 329, 529 (1987)
3. A. Melker, S. Romanov and D. Kornilov, *Matter. Phys. Mech* 2, 42-50 (2000)
4. A.T. Werner, J. Anders, H.J. Byrne, W.K. Maser, M. Kaiser, A. Mittelbach and S. Roth, *Appl. Phys. A*, 57, 157. (1993)
5. R. Haddon *Acc. Chem. Res.* 25 127 (1992)

6. E. Mele and S. Erwin *Phys. Rev. B* 50, 2150–8 (1994)
7. S. Satpathy, V. Antropov, O. Andersen, O. Jepsen, O. Gunnarsson and A. Liechtenstein, *Phys. Rev. B* 46, 1773 (1992)
8. M. Gelfand and J. Lu, *Phys. Rev. Lett.* 68, 1050 (1992)
9. M. Gelfand and J. Lu, *Phys. Rev. B* 46, 4367 (1992)
10. M. Gelfand and J. Lu, *Phys. Rev. B* 47, 4149 (1993)
11. S. Phelan, MPhil Dissertation, Dublin Institute of Technology (2004)
12. P. A. Heiney, J. E. Fischer, A. R. McGhie, W. J. Romanow, A. M. Denenstein, J. P. McCauley Jr., A. B. Smith III, and D. E. Cox, *Phys. Rev. Lett.* 66, 2911-2914 (1991).
13. M. Dresselhaus, P. Eklund, *Science of Fullerenes and Carbon Nanotubes*, Academic Press Inc. London (1995)
14. J. Fischer and P. Heiney, *J. Phys. Chem. Solids* 54, 1725 (1993)
15. G. Chambers, PhD Dissertation, Dublin Institute of Technology (2001)
16. L. Akselrod, H.J. Byrne, J. Callaghan, A. Mittelbach and S. Roth, in *Electronic Properties of Fullerenes*, H. Kuzmany, J. Fink, M. Mehring and S. Roth eds., *Springer Series in Solid State Sciences*, Springer Verlag Heidelberg, 117, 219 (1993)
17. S. Kazaoui, N. Minami, Y. Tanabe, H.J. Byrne A. Elimes, P. Petelenz, *Phys Rev B.* 58, 7689, (1998).
18. G. Bublitz, S. Boxer, *Annu. Rev. Phys. Chem.* 48, 213 (1997)
19. A.M. Rao, P. Zhou, K.A. Wang and P.C. Eklund. *Science*, 259, 955. (1993)

Chapter 3

SAMPLE PREPARATION AND EXPERIMENTAL
METHODS

3.1 Film production

For this study, films of C_{60} electrically contacted in a geometry accessible for in situ optical characterisation were required. Thin films of C_{60} have been prepared by many different techniques such as molecular beam epitaxy, vacuum evaporation and hot wall epitaxy. In this case vacuum sublimation was used as it provides several advantages over the other methods such as simplicity, large area coating capability and deposition without destroying the C_{60} structure. Vacuum sublimation is known to produce high optical quality fullerene films of thickness in the range 10 nm-1 μm [1,2]. The films are polycrystalline consisting of domains which grow from the substrate plane. As transport within these individual domains rather than between domains is of primary interest, a sandwich rather than an in plane electrode geometry was chosen. To facilitate in situ optical characterisation, a transparent bottom electrode is desirable.

The substrates used were glass slides coated with indium tin oxide, commonly known as ITO. A coat of clear nail varnish was placed over the slides leaving only one small part of the electrode exposed. When the nail varnish was dry the substrates were placed in boiling HCL for 10-15 seconds to etch away the exposed part of the electrode. The resistance across the etched part was then tested using a multimeter. For pure glass the surface resistance should be of the order of mega Ohms. The substrates were placed in a beaker of acetone and then sonicated for a few minutes to dislodge the nail varnish. This allowed for films to be produced in a sandwich type geometry. Films of C_{60} were prepared by vacuum sublimation onto the indium tin oxide substrates. The substrates were mounted onto a metal plate, coated face down, located above the sample in the vacuum chamber. The ITO layer was used as the bottom electrode. The C_{60} was vapour

deposited onto the substrate using the Edwards Auto 306 evaporation system illustrated in Figure 3.1. The evaporation chamber was sealed and pumped down to about 10^{-6} mbar and with the addition of liquid nitrogen to the system, the chamber was evacuated to a pressure of 10^{-7} mbar. The shutter located between the sample and the substrate was closed so as to protect the substrate from being contaminated by any impurities.

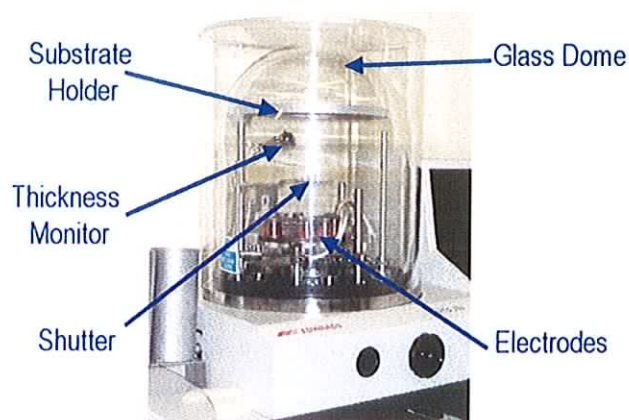


Figure 3.1: Picture of Edwards Auto 306 evaporation system

A molybdenum boat containing 5 mg C_{60} powder was connected to the positive and negative terminals of the power supply and then resistively heated by slowly passing a current through it. When the current reached a value of approximately 40 amps the shutter was opened and the C_{60} was sublimed onto the surface of the substrate. The current was slowly increased to about 60 amps, this process continued until a desirable thickness was achieved. As the evaporation process took place the pressure and temperature of the sublimation were both monitored to ensure the formation of a homogeneous film. A layer of aluminium (~200 nm) was then evaporated on top of the C_{60} to form the top electrode. The system was allowed to cool for approximately half an

hour whilst maintaining low pressure after which the chamber was vented. This cooling period prevented oxides or other contaminants forming on the surface of the films. Some of the films were then transferred to the laminar fume cupboard in tin foil so as not to contaminate them with any dust/dirt particles in the air. They were then stored in a nitrogen atmosphere until tests were ready to be carried out; this was done to ensure as little contact with the air as possible. Unfortunately the container used was not air tight and so after some time the nitrogen can leak out allowing air particles into the storage container. A way of overcoming this would be to seal the rim with vaseline or used a heavy gas such as argon.

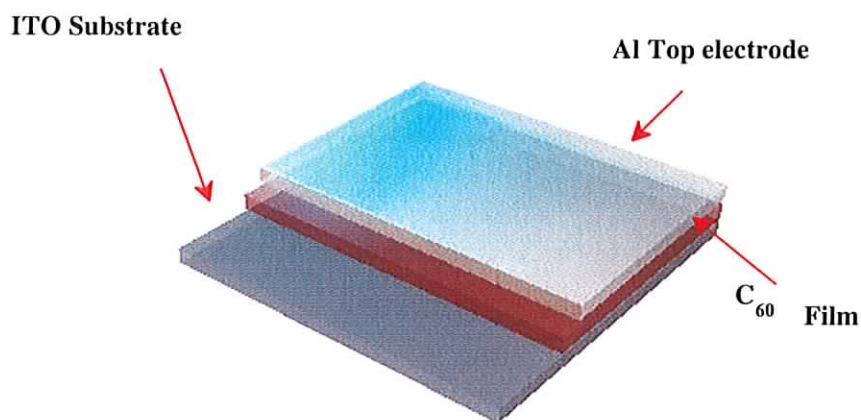


Figure 3.2: ITO/C₆₀/Al sandwich structure

3.2 Thickness Determination

The thickness of the films produced was measured using the Dektak³ surface profilometer with an accuracy of $\sim 50 \text{ \AA}$. The purpose of the Dektak³ is to give a quantifiable measurement of the surface profile of a sample. It can be used to measure the height or width of a feature on the surface of the sample, such as a small etches, a metal deposit, or

the thickness of a resist. The profile can also give a look at the roughness of the surface in order to ascertain a uniform thickness. The profilometer operates by lightly dragging a sharp, diamond tipped stylus over the surface of the substrate and recording the vertical profile of the surface. A diamond stylus is moved vertically into contact with the sample and then moved laterally across the sample for a specified distance and specified contact force. The instrument can measure small surface variations in vertical stylus displacement as a function of position. The Dektak³ profilometer can measure small vertical features ranging in height from 100 Å to approximately 650,000 Å on a 12.7 cm Diameter Sample Stage. The height position of the diamond stylus generates an analogue signal, which is converted into a digital signal, stored, analyzed and displayed. The radius of the diamond stylus is roughly 12.5 μm, and the scan speed and length of the scan control the horizontal resolution. There is a horizontal broadening factor, which is a function of stylus radius and of step height. This broadening factor is added to the horizontal dimensions of the steps.

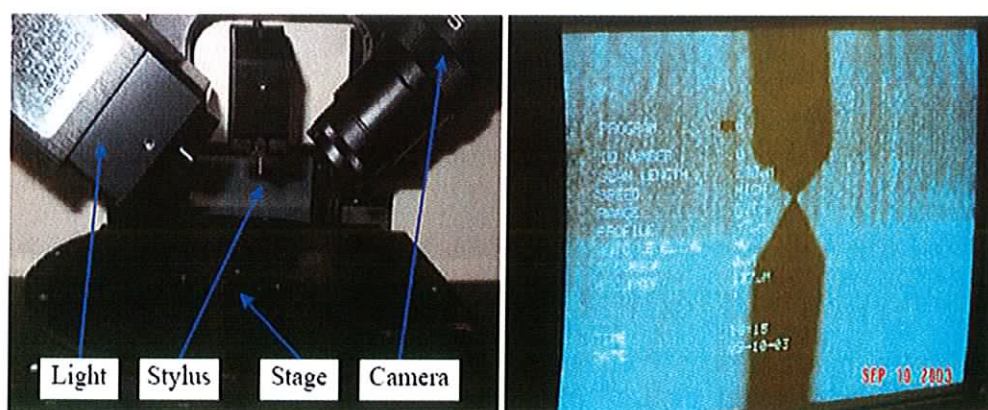
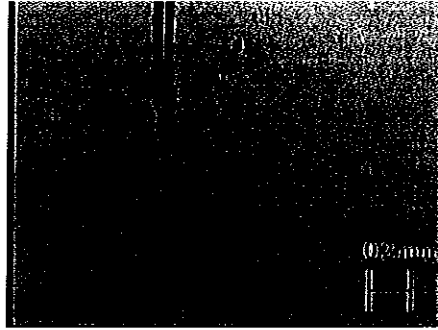


Figure 3.3: Dektak³ profilometer scanning hardware (left) and video output (right)

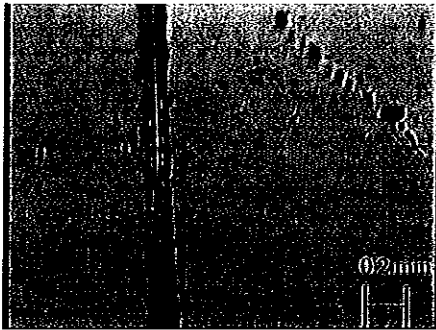
3.3 Dektak³ Method

A sample is mounted onto the stage, which can be adjusted until a clear part of the surface is visible to measure. A small scratch is etched onto the surface of the film using a sharp blade so that a straight edge is obtained. The image is focused using the large or coarse focus knob on the side of the machine. When a clear part of the surface is obtained and focused, the scratch is positioned so as they are parallel on the screen. The needle/stylus can be positioned using the display/sample-positioning icon on the tool bar. The stylus is the dropped down onto the surface of the sample and a scan is taken. The diamond tipped stylus moves across the surface of the sample. After it passes the scratch on the surface the escape key is pressed to stop the program running.

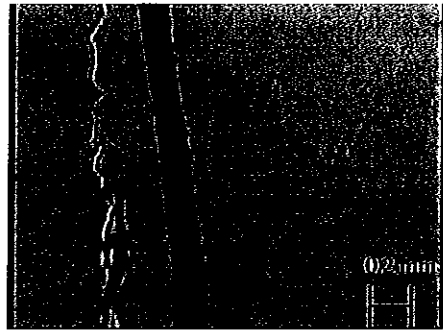
The distance between the surface of the electrode and the glass can then be determined using the cursor keys. The graph can then be analysed to show the drop in height from the surface of the film to the substrate. Figure 3.4 below shows images of various thicknesses of thin films of C₆₀ from the Dektak³. They show reasonable even surfaces with no pinholes. Small amounts of dust may gather on the surface when measurements are being carried out so it is imperative that the scans do not run for too long to reduce exposure of the films.



(a)



(b)



(c)

Figure 3.4: Scratch on the surface of a film of (a) 218 nm, (b) 501 nm and (c) 814 nm thick

3.4 Spectroscopic Characterisation

Spectroscopy is the use of the absorption, emission or scattering of electromagnetic radiation by matter to qualitatively, or quantitatively, study the matter and its physical processes. The interaction of radiation with matter can cause redirection of the radiation and/or transitions between the energy levels of the constituent atoms or molecules. Matter can capture electromagnetic radiation and convert the energy of a photon to some form of energy, for example internal energy [3]. This process is known as absorption and this type of spectroscopy is just one way of studying the energy levels of the molecules.

Optical (UV/visible) spectroscopic characterisation of the films was carried out using the Perkin Elmer Lambda 900 UV/VIS/NIR spectrometer. This is a double beam, double monochromator ratio recording system, which utilises two pre-aligned light sources. The first is a deuterium (D_2) lamp for the ultraviolet light and there is also a tungsten (W) lamp for the visible light. The wavelength range is from 175 nm to 3300 nm with an accuracy of 0.08 nm in the UV-visible region and 0.3 nm in the NIR region.

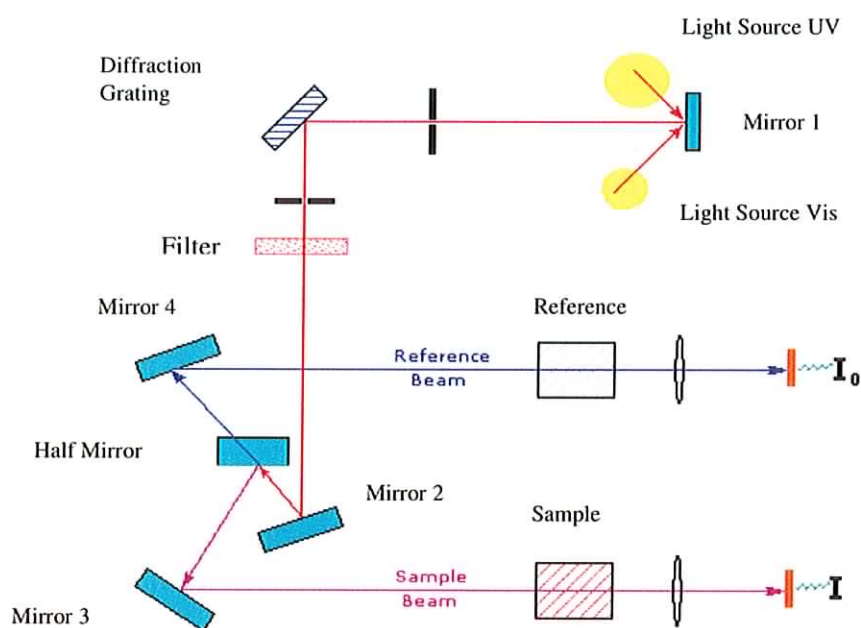


Figure 3.5: Internal workings of UV/Vis spectrometer

Figure 3.5 presents a schematic layout of the optical system. The light beam bounces off mirror 1, it then passes through a slit and hits the diffraction grating. The grating can be rotated allowing for a specific wavelength to be selected. At any specific orientation of the grating, only monochromatic light successfully passes through the slit. A filter is

then used to remove unwanted higher orders of diffraction. The light beam hits a second mirror and is deflected to a half mirror, where half of the light is reflected and the other half passes through. One of the beams is reflected to the sample itself and the other passes through the reference sample. The intensities of the light beams are then measured at the end.

One advantage of using absorption spectroscopy as a measurement technique is that the Beer Lambert law defines a simple linear relationship between the spectrum and the composition of the sample. Simply stated the law claims that when a sample is placed in the beam of a spectrometer there is a direct and linear relationship between the amount of it's constituents and the amount of energy it absorbs. The general Beer Lambert law is usually written as:

$$A = \epsilon c b.$$

Equation 3.1

where A is the measured absorbance, ϵ is the wavelength dependant absorption coefficient, c is the concentration and b is the pathlength.

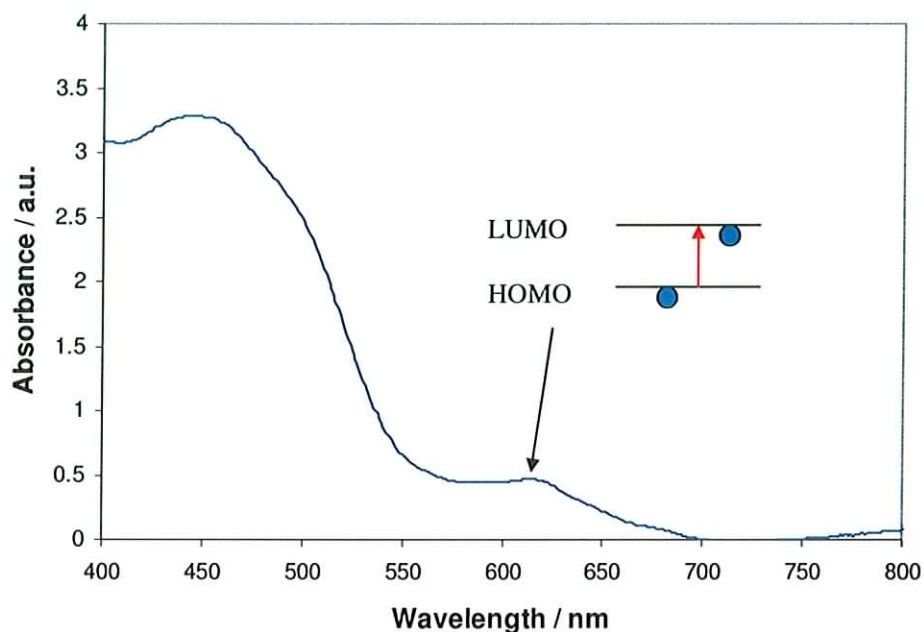


Figure 3.6: Absorbance spectrum of film 500 nm on glass substrate

Figure 3.6 shows the absorption spectra obtained for a deposited film of 500 nm thick. As discussed in Chapter 2 the predominant peaks, at 445 nm and 615 nm, are clearly evident. The peak at 445 nm is attributed to intermolecular charge transfer. The peak at 615 nm is the HOMO-LUMO transition as observed in the solution spectrum (Figure 2.8). Again in Chapter 2 a comparison of solution and solid state is discussed, and shows that the feature at 445 nm is not present in the solution spectrum and so it can be determined that this is evidence of the first solid state feature arising. It should be emphasised again that as this feature derived from intermolecular interaction it is strongly dependent on morphology and can be used as an indicator of the solid state.

3.5: Electronic Characterisation

The system used consisted of a computer, which utilised a LabVIEW program, a Keithley 237, which is a programmable electrometer, and a cryostat chamber. A temperature controller was attached to the cryostat so at any given time the temperature of the chamber could be noted. The end of the cold finger in the cryostat contained a sample holder to fix the sample in place whilst the readings were being taken. Firstly, in order to obtain true IV characteristics of the C_{60} films the set up used was initially characterised so as to show that the system was in working order. IV curves were run at various stages of the set up both in open circuit and with a load resistor.

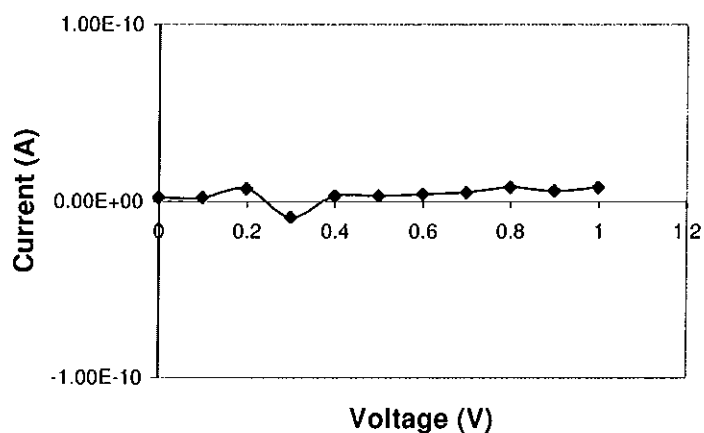


Figure 3.7: Open circuit characterisation graph of set up

In Figure 3.7 the open circuit current-voltage plot is shown. This plot was taken directly from the Keithley electrometer. The leads extending from the meter were connected to the cold finger with the sample holder at the end open and empty. The voltage was set to run from 0 volt to 1 volt. At increments the current was recorded and plotted to show that

there was no short circuit in the set up. As can be seen from the Figure 3.7 the noise level is $<1 \times 10^{-11} \text{A}$ at 1V, and as this is quite low it should not affect the results acquired.

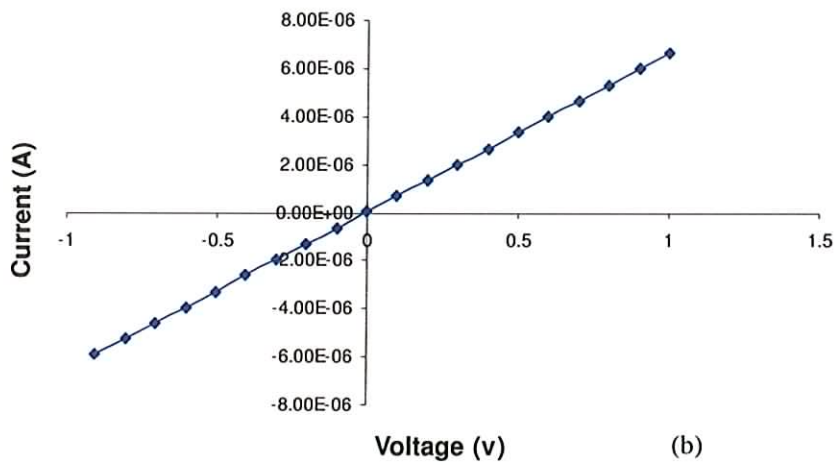
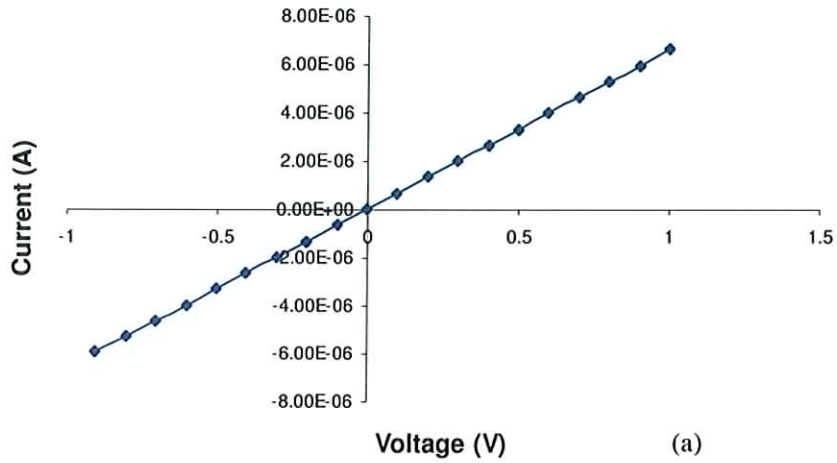


Figure 3.8: Load resistor characterisation graphs (a) external to and (b) within the cryostat.

To further characterise the set up the circuit was connected to a load resistor of $150 \text{ k}\Omega$. Again the resistor was connected directly to the output of the Keithley (Figure 3.8a) and

within the sample holder (Figure 3.8b). Both graphs gave a value of $1.51 \times 10^5 \Omega$, which correlates with the known value of the resistor. This suggests that the system was running efficiently and that there were no discrepancies with the internal circuitry.

3.6 Testing of films

The solid-state electrical measurements were conducted in a cryostat. Initially silver conducting paint was used on top of the aluminium layer as it was thought to make good electrical contact with the film.

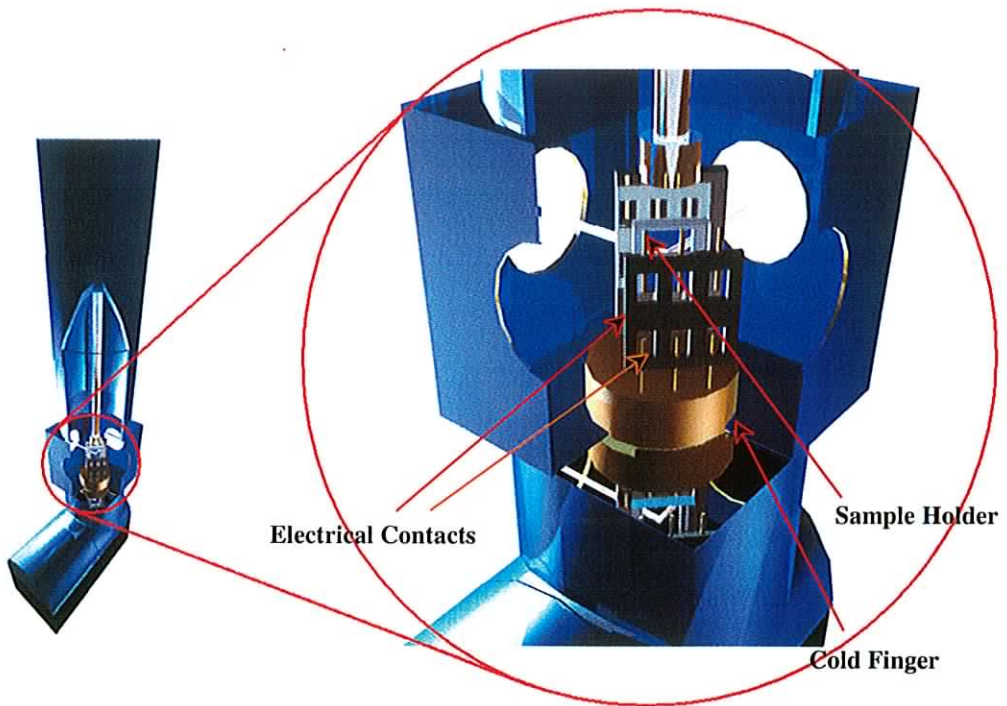


Figure 3.9: Experimental set-up showing Oxford Cryostat and sample holder for films [2].

Silver was used as it is considered to be the best conductor as it has a low specific resistivity, crystallises easily and also has an ohmic response to a voltage input. The films were placed in the sample holder at the end of the cold finger and then inserted into the cryostat; the chamber holding the sample was evacuated. Current voltage graphs of the films were then obtained by connecting the Keithley 237 programmable electrometer to the cryostat. Liquid nitrogen was then added to the system so that low temperature measurements could be acquired. When the desired temperature was reached the IV characteristics of the sample could be directly measured.

The graphs obtained were then analysed and the conductivity of the films was determined. Finding the slope of the graph and using the equation below the conductivity of the films could be found.

$$\text{Conductivity} = (1/\text{Resistance}) \times (\text{Thickness}/\text{Area}) \quad \text{Equation 3.2}$$

where $1/\text{resistance}$ is equal to the slope of the graph.

The use of the silver conducting paint proved to be detrimental to the film over prolonged periods of time as it etched into the film. In turn this gave graphs that seemed to be 'short circuit' rather than the desired conductivity graphs for the fullerene films. In order to eliminate this problem the silver conducting paint was removed. The original sample holder was made of a square piece of plastic in which the films were slotted. Electrical contacts were wired from the cold finger to a "Sim card" holder at the end. They were then placed in contact with either end of the film and held in place using plumbers tape. Unfortunately this did not seem to make good electrical contact

with the films and so a new sample holder was created. The new holder encompassed a door like latch, which allowed the film to be held in close contact with the prongs of the Sim card holder.

3.7 Summary.

This chapter described the production of the thin films of C_{60} and also the techniques for spectroscopic and electrical analysis. Initially the substrate preparation is discussed followed by the sublimation process. The thicknesses of the films were then determined using the Dektak³ profilometer. Spectroscopic characterisation gives insight into the electronic configuration and also reveals any features specific to the solid. The electronic set up was characterised in order to show that the films would have sufficient contact so that all future measurements are as accurate as possible. Solid state measurements are described, in which the Keithley 237 electrometer is employed. In the following chapters the variation of both the optical and electronic properties of the films produced under differing conditions will be described and examined.

References

1. G. Chambers, PhD Dissertation, Dublin Institute of Technology (2001)
2. S. Phelan, MPhil Dissertation, Dublin Institute of Technology (2004)
3. R. Thatipamala, G. Hill and S. Rohani, *J. Chem. Eng.* 71, 977 (1993)

Chapter 4

SPECTROSCOPIC ANALYSIS

4.1 Introduction

In thin film production there are numerous factors which may affect the solid-state properties of the fullerenes, the most common of these being annealing. This is a process whereby the films are heated and cooled slowly. Annealing can alter the microstructure of a material causing changes in properties such as strength and hardness. In fullerene films it can be used to control charge transfer and increase the conductivity of the pristine material [1, 2]. However, for a fundamental study of the properties of solid state fullerenes, including the effects on charge injection on the electronic properties, unannealed films are desirable.

To minimise annealing effects the substrate holder was kept at a maximum distance (~15 cm) from the sample. This was to ensure that the film being deposited was subjected to as little heat as possible. It has been shown in previous reports that this distance between substrate and evaporation boat plays a large part in annealing the films [1]. In order to achieve as close to a true molecular insulator as was possible the substrate/boat distance was kept at a constant maximum distance.

4.2 Film Analysis

Films were deposited for varying exposure times, between 5 and 60 minutes, and the thickness monitored using the Dektak³. In all the films produced 5mg of sublimate (C₆₀) was used. Also the temperature of the sublimate was monitored so as to keep the preparation conditions uniform. Figure 4.1 shows the film thickness against time for deposition from an evaporation boat of area $8.85 \times 10^{-5} \text{ m}^2$. If we look at this thickness

versus time in it can be seen that there is an expected trend. The thickness of the films is seen to increase although not exactly linearly. Given the accuracy of the Dektak³, (± 5 nm) this deviation from linearity is unexpected. At short times, fluctuations in thickness would be expected, as there is what is known as an incubation period. This is the time it takes to form a full layer on the surface of the substrate. This layer does not always form evenly straight away; it may start in columns and grow outwards. Between a time of 15 and 30 minutes there is an increase in thickness of roughly 80 nm. A sublimation time of 60 minutes was required to reach a thickness of 800 nm. This is a long time to expose both the C_{60} in the boat and in film form to high temperatures inside the chamber. During the evaporation process the volume of sublimate was kept constant (5 mg) and the boat temperature was monitored.

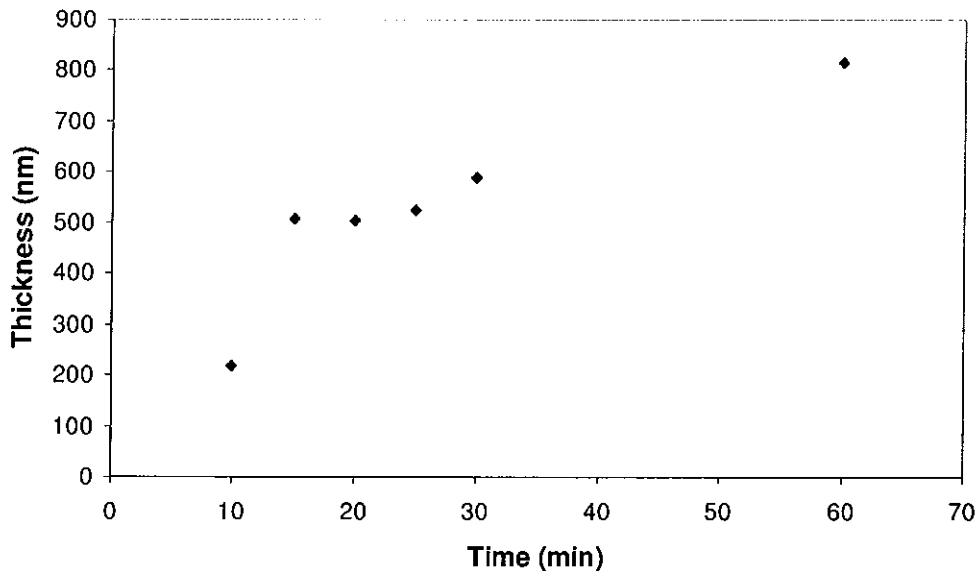


Figure 4.1: Thickness against time for a range of films

The absorption spectra of the range of films produced under these conditions are shown in Figure 4.2. As discussed in previous chapters the HOMO-LUMO transition is evident at 615 nm although this peak decreases as the thickness of the films decreases. Interestingly the charge transfer peak at 445 nm is relatively flat and broad in comparison to the absorption spectrum in Chapter 3 (Figure 3.6). This type of spectrum is more comparable to that of the annealed films more so than pristine [1]. These changes in the spectra can be due to a number of issues, the most common of these being the aforementioned annealing.

Also, there is a residue of C₆₀ left in the boat, which could be deposited on the films as the material is being sublimed. This residue is insoluble in organic solvents and has been speculated to be polymerised C₆₀ [3]. Contamination of the films with evaporated polymer will affect the molecular structure of the C₆₀ lattice. Another factor that may cause a reduction in peak intensity could be due to oxygenation [4]. Given the large amount of interstitial volume in the solid C₆₀ structure, molecular oxygen from the air readily diffuses into the solid thus creating deep electronic traps [5]. The more oxygen present in the C₆₀ lattice the deeper these traps may become.

Aluminium diffusion may also pose problems as the amount of diffusion is not known. As the aluminium molecules move deeper into the film they reduce the path length of the electrons and effectively the measured thicknesses are not the same as the distance travelled through the material. This in turn then affects the conductivity results obtained. In this study the aluminium layer was kept fairly thin so as any diffusion maybe considered negligible in comparison to the film thickness. A further study should be done on the diffusion process in order to fully ascertain the affect on the film

conductivity. The crystallinity of the fullerene films needs to be improved so as not to hinder their optical and electronic properties.

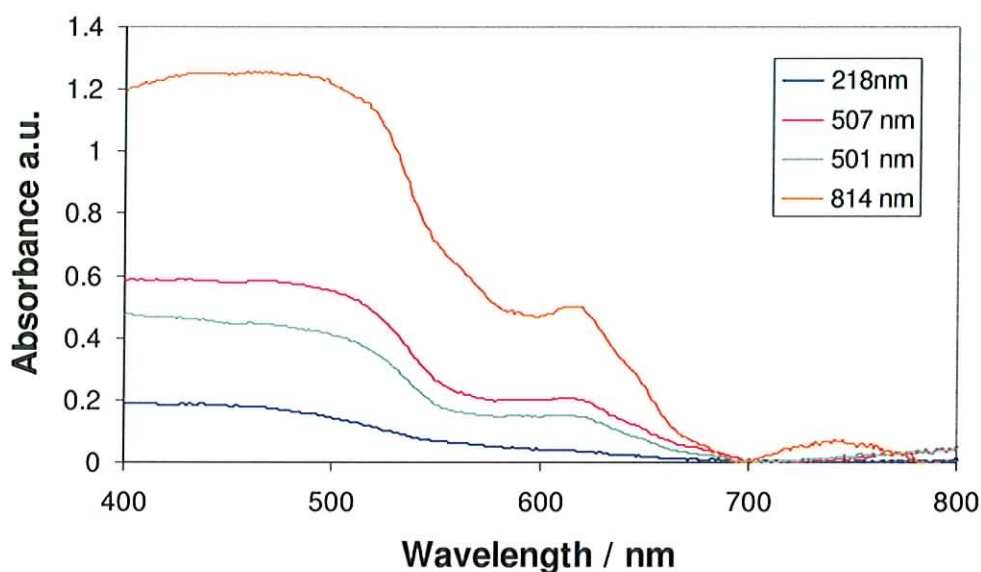


Figure 4.2: Absorbance spectra for a range of films

Given a morphology which is independent of deposition time, the absorption of the films should be linearly dependent on the measured thickness, in accordance with the Beer Lambert law. However this did not seem to be the case in this study. Each of the films produced was spectroscopically characterised using the UV/Vis and the maximum absorption peak at 445 nm, which has been attributed to intermolecular charge transfer, was noted and plotted against the thickness of the films deposited. As seen from Figure 4.3, a linear trend was not observed. The reproducibility of any individual spectrum is within 1% and so the variability does not derive from instrumental factors. The films produced showed no repeatability in their spectral characteristics suggesting the morphologies of the films were not reproducible. These results led to questions as to

the production method and so a more suitable way in which to produce thin films of C_{60} with pristine characteristics should be found.

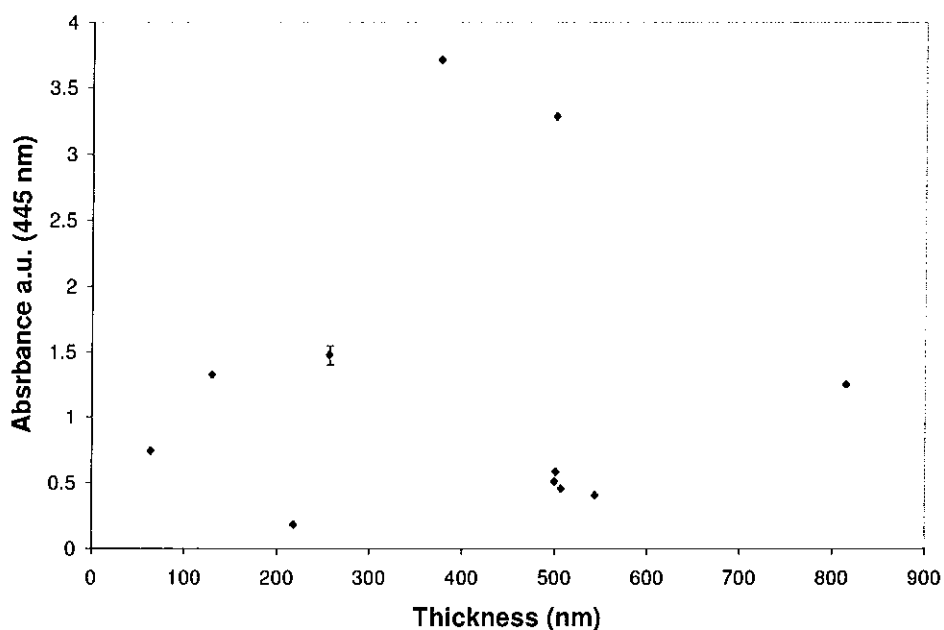


Figure 4.3: Absorption (at 445 nm) versus thickness of films

Noting the relatively slow deposition rate of Figure 4.1, the deposition rate of the films was varied. To do this, three molybdenum boats of different areas were used. During the evaporation process the sublimation time for each boat was noted along with the thickness of the film produced and the corresponding absorbance. The results shown above were obtained from the first boat used. This evaporation boat had a small surface area, which in turn yielded a slow deposition rate. Table 4.1 lists the dimensions of the three deposition boats employed.

Table 4.1: Dimensions of evaporation boats employed

Boat	Length(m)	Width(m)	Depth (m)	Area (m ²)
1	9.68×10^{-3}	9.14×10^{-3}	3.16×10^{-3}	8.85×10^{-5}
2	13.54×10^{-3}	6.48×10^{-3}	2.42×10^{-3}	8.77×10^{-5}
3	23.08×10^{-3}	9.96×10^{-3}	1.62×10^{-3}	2.29×10^{-4}

A comparison between both the slow and fast deposition rate shows how changing the smallest of parameters can affect the films produced. As the surface area of the boat is decreased the deposition rate of the fullerenes becomes slower. Table 4.2 lists the results obtained for the three different deposition rates. Looking at boat three it can be seen that in a 10-minute period, from 15 to 25 minutes, the thickness increases by a substantial amount, over 200 nm, whereas, as previously mentioned, for the slower deposition, a 15-minute period produces films with only 80 nm difference in thickness.

Figure 4.4 shows how the evaporation times varied for the three different boats and the impact this had on the film thickness. For example if we look at an evaporation time of 25 minutes, boats 1 and 2 produced films of similar thicknesses although boat 2 is more consistent and linear in the thicknesses produced. The third boat produced a film nearly 300 nm thicker in the same time. This implies that the larger surface area has a substantial affect on the thickness of the films. A larger surface area means that the molecules can sublime almost simultaneously as they are in direct contact with the boat itself. The other boats had deeper “wells” which means that molecules at the bottom had to supply energy to the next layer of molecules and so on until the top layer

acquired enough energy to sublime. The larger area boats 2 and 3 also exhibit a more linear dependence of thickness produced versus deposition time.

Table 4.2: Evaporation time, thickness and absorbance of films produced from three different boats

Time (min)	Boat 1		Boat 2		Boat 3	
	Thickness (nm)	Absorbance @ 445 nm	Thickness (nm)	Absorbance @ 445 nm	Thickness (nm)	Absorbance @ 445 nm
5			63	0.74		
10	218	0.18	130	1.13	375	2.40
12					413	3.09
15	507	0.45	257	1.47	581	4.35
18					648	4.87
20	501	0.58	376	3.71	704	5.03
25	523	0.61	500	3.28	803	5.64
30	589	0.66				
60	814	1.25				

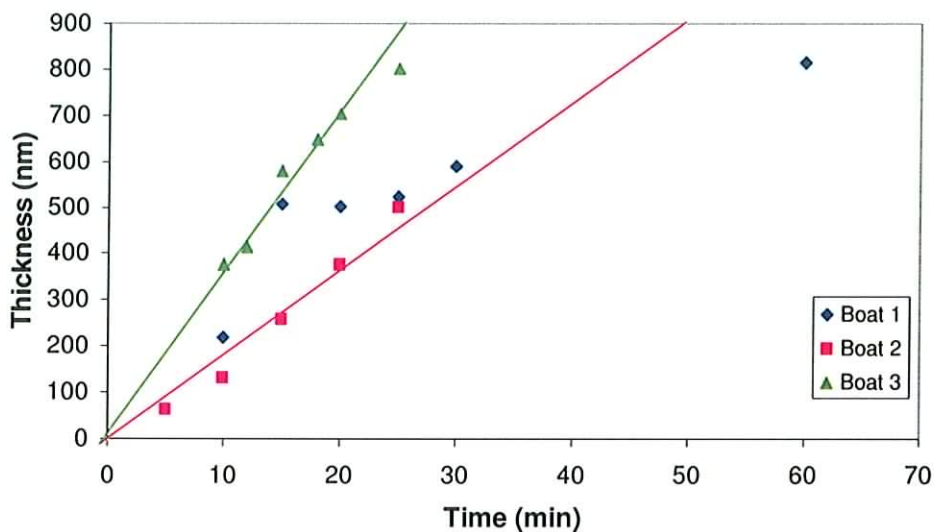


Figure 4.4: Shows thickness versus time for different boats

Previously the small boat area ($8.85 \times 10^{-5} \text{ m}^2$) has been examined and analysed showing that the films produced vary significantly in morphology. If the plot of absorbance versus thickness is looked at, for a deposition from a boat area of $2.29 \times 10^{-4} \text{ m}^2$ a more linear relationship in accordance with the Beer Lambert law is observed. As can be seen from Figure 4.5, the absorbance is increased as the thickness increases.

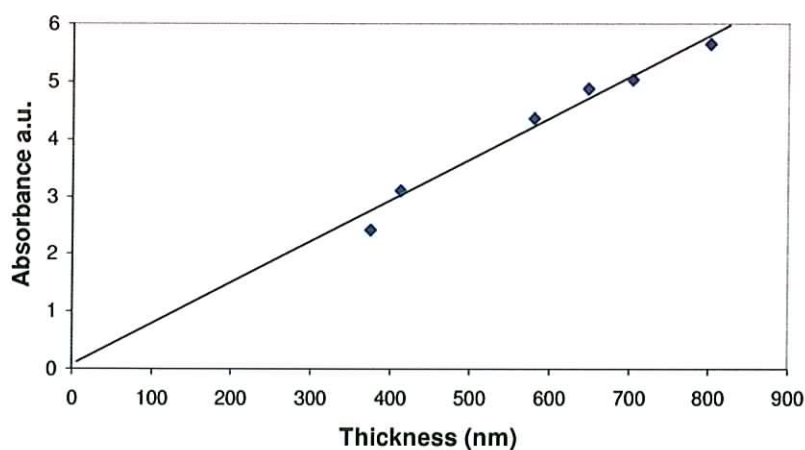


Figure 4.5: Absorbance against thickness for a range of films from boat 3

If we look at how these different deposition rates have affected film morphology as determined by optical spectroscopy, as shown in Figure 4.7, we see that the fast deposition (boat 3), which has the larger surface area, was the best for producing films of similar morphologies. As can be seen from the spectra below the HOMO-LUMO transition is clearly evident as is the intermolecular charge transfer at 445 nm. The intensity of the absorbance changes due to the film thickness and the thicker films have a much more defined peak at 445 nm.

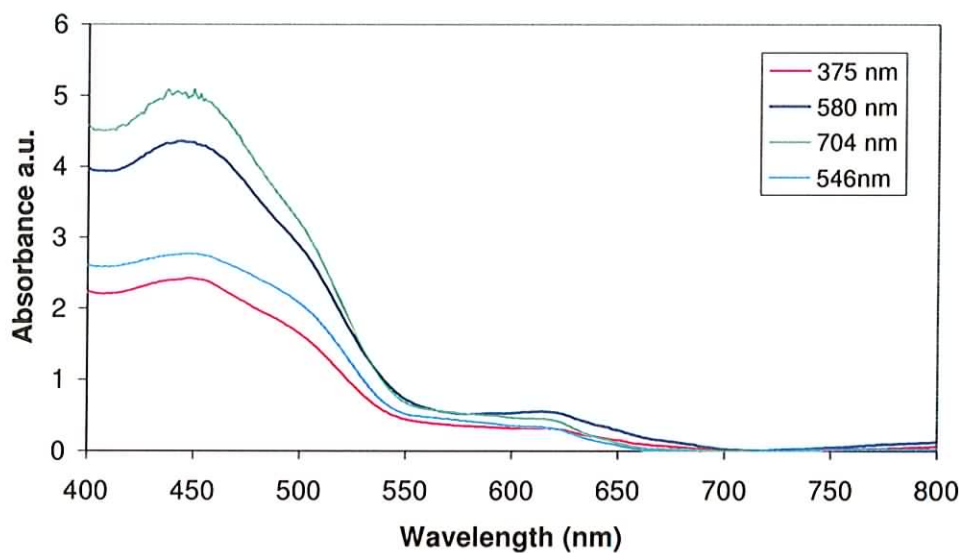


Figure 4.6: Absorbance spectra for a range of films (smaller boat area)

4.3 Summary

Firstly it was noticed that slow deposition rates yielded poorly defined optical absorption spectra. Spectra obtained more closely resemble those of annealed films. It is concluded that in the small area boats, the material not free to sublime from the

evaporation boat is subjected to significant heating resulting in polymerisation and or annealing. The films produced are therefore of a variable morphology and there is no correlation between the absorption and the film thickness. Use of a larger boat area results in more rapid deposition. The absorption spectra observed are consistent with literature for unannealed pristine C₆₀ films and the absorption is well correlated with film thickness. Given the variation in film morphology, it is anticipated that that electronic properties of the films produced by the different methods will be similarly varied. This is explored in the following chapter.

References

1. S. Phelan, MPhil dissertation, Dublin Institute of Technology (2004)
2. G. Farrell, PhD dissertation draft, Dublin Institute of Technology (2006)
3. G. Meijer, private communication (2006)
4. A. Assink, J. Schirber, D. Loy, B. Morosin and G. Carlson, *J. Mat. Res.* **7**, 2136 (1992)
5. B. Pevzner, A. Hebard and M. Dresselhaus, *Phys. Rev. B* **55**, 16439 (1997)

Chapter 5

ELECTRONIC ANALYSIS

5.1 Transport processes in molecular materials

Electrical conductivity is the measure of a material's ability to conduct an electric current. Insulators have a low conductivity whereas metals, which are known as conductors, have relatively high conductivities. Molecular solids are made-up of discrete units, which are typically bound by weak van der Waals forces, in which the electrons are localised. The conductivity of the material is dependant on the band gap of the material which is the minimum energy required to promote an electron into the conduction band of the material. Within conjugated systems, the electrons can have high mobility but at the same time require energy to make the transition to another molecule. Organic molecular solids can be either amorphous or crystalline (as in the case of fullerenes). In these systems the process of intermolecular transport can be very complex. In the majority of cases the electron transport is almost a hopping-like process and can be thermally activated [1].

In molecular systems where conductivity is dominated by thermally activated hopping, the electrons that carry current through the material are generally bound in potential wells resulting from defects or impurities. Collectively these defects are known as traps. In the case of crystalline molecular materials these traps are the molecules themselves, as the electrons that are bound in them need energy before they can move to the next molecule and so on. For example, consider that the electrons require an energy (Δ) to escape from the traps; if the electrons are supplied with a thermal energy (Δ) equal to that of the trap energy then they can essentially escape and move through the substance carrying a current. Along the way they may fall into yet another trap in the lattice and the process starts again until a conduction channel has been created through

the material. This hopping mobility is usually characterised by an increase in current with an increase in temperature. The electrical conductivity (σ) in these situations is roughly proportional to the probability that the electrons can acquire enough energy to escape the traps [2]. When predicting whether a solid is an insulator or not it is important to look at band overlap which is dependant on the geometry of the crystal structure. If a completely filled valence band overlaps with a completely empty band then two partially filled bands are produced, this results in a solid that might have originally been an insulator becoming conducting. At temperatures above 0 Kelvin it is possible for some electrons to gain enough thermal energy to overcome the energy gap. The probability of this happening increases with temperature and depends strongly on the width of the energy gap. This trap energy is a characteristic property of the molecule and the lattice packing. The temperature dependant electron transition is known as thermally activated hopping transport and is characterised by the behaviour as described by equation 5.1. [3]

$$\sigma = A \exp(-\Delta/kT) \quad \text{Equation 5.1}$$

where σ is the conductivity, A is a constant and T is the temperature and k is the Boltzman constant. Thus at constant voltage this equation can be written as:

$$I(T) = I(0)\exp(-\Delta/kT) \quad \text{Equation 5.2}$$

where I(T) is the current at temperature T. Thus, for a crystalline material with a single activation energy Δ , a plot of $\ln(I)$ versus inverse temperature should yield a straight line of slope $-\Delta/k$.

The electronic properties of solid-state fullerenes are critically dependant on the local environment and also the crystal packing [4]. In polycrystalline films the conductivity is limited by polycrystalline domain boundaries. Typically conductivity values have been reported for pristine C_{60} are of the order of $10^{-10} \text{ S cm}^{-1}$ [4]. However, this conductivity can be strongly dependent on film morphology and effects such as oxygen inclusion [5] and annealing [6]. Given the variability in the spectroscopic characteristics of the films produced by differing deposition rates, it is expected that the electrical properties of the films will be similarly varied.

In order to examine the transport processes in the films produced under the different conditions, films of similar thickness, 589 nm and 581 nm produced from boats 1 and 3 respectively were chosen. To perform the temperature dependence of the conductivity the films were mounted in the Nitrogen cold finger as described in Chapter 3 and a voltage of 1V was applied. As the temperature was increased from 77 K to 295 K, in increments of 5 K, the corresponding current was noted using the Keithley 237 electrometer.

Figure 5.1 illustrates the temperature dependence of the current for the two films. Looking at plot (a) it can be seen that there is an increase in current as the temperature increases, characteristic of a thermally activated hopping conductivity. A hopping activation energy of 3.6meV can be ascertained from the slope of the graph. These values are not consistent with those reported for pristine fullerene films. The range of reported activation energies is very wide (0.3 eV to 1.1 eV) [5]. This variation can be attributed to the geometry in which the measurements are obtained.

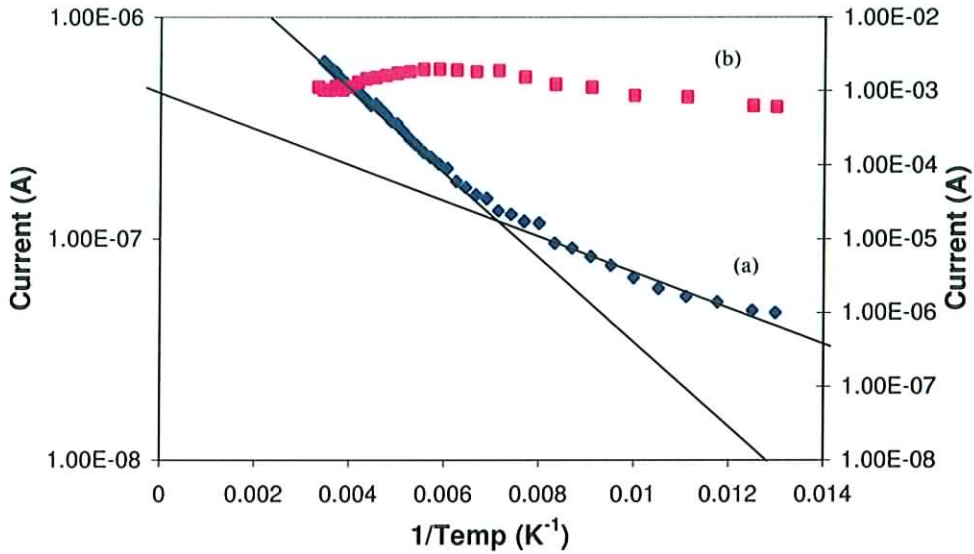


Figure 5.1: Temperature dependence of the measured current at 1V for films of thickness 589 nm produced by boat 1 (b), plotted on x and secondary y axes, and 581 nm produced by boat 3 (a), plotted on x and y axes.

In this study the measurements are taken in a sandwich type geometry whereas previously they have been done in a planar geometry. In a planar type of geometry the conductivity is limited by the polycrystalline domain boundaries and hence a higher activation energy is required. In the sandwich geometry it is thought that the conduction is through a crystalline column and so no interdomain hopping is needed. However at a particular temperature ($\sim 130\text{K}$) the rate at which the current increases changes. Such a deviation has previously been observed in fullerene films [7] and has been attributed to the onset of molecular rotations at the phase transition temperature (as described in Chapter 2). The activation energy above the transition temperature is much higher than below ($\sim 13.1\text{ meV}$). This therefore implies that the intermolecular hopping energy is increased above this temperature. This corresponds to the fact that at higher

temperatures there is a decrease in intermolecular mobility due to rotational motion. In Figure 5.1(a), the temperature at which this change occurs is much lower than the known phase transition temperature (249K), however. A potential explanation of this difference is due to resistive heating, whereby the temperature of the film is significantly higher than that of the cold finger heat sink. This can be estimated by considering the electrical power, $P=VI$. A voltage of 1V produces a current of $10^{-7}A$ this is calculated to be $10^{-7} W$. This power can then be transformed into a temperature change by using the following equation.

$$\Delta T = (Q \times d) / (tA\kappa) \quad \text{Equation 5.3}$$

where Q is the energy, t is the time, d is thickness, A is area and κ is the thermal conductivity. As energy over time is power the equation can be written as [8]:

$$\Delta T = (\text{Power} \times d) / (A\kappa) \quad \text{Equation 5.4}$$

From literature the value for thermal conductivity is $0.4 \text{ Wm}^{-1}\text{K}^{-1}$ for polycrystalline fullerenes [9]. When considering the whole area of the film ($4.8 \times 10^{-3} \text{ m}^2$) the temperature difference is calculated as $\Delta T = 3 \times 10^{-11} \text{ K}$. If however the conductivity is through 1 micro crystallite with an area of approximately 10^{-12} m^2 then $\Delta T \sim 1 \text{ K}$. This corresponds to a temperature which could not account for a discrepancy of $\sim 120 \text{ K}$. An alternative explanation is that the behaviour is not best defined by a single (or double) activation energy, characteristic of crystalline materials, but rather that there are a range of different activation energies, and the transport mechanism is better described as a variable range hopping process.

5.2 Variable range hopping

In non-crystalline molecular solids the electrons that carry the current through the material are in a random potential. This means that spatially the potential energy moves up and down randomly. As the electrons navigate through the material they are drawn to dips in the potential energy, known as potential wells, and at low temperatures they can move through the system by hopping to adjacent potential wells. Unlike thermally activated hopping there is no single activation energy that defines this system. This variable range hopping has a very distinctive temperature dependence given by [10]:

$$\sigma = C \exp(D/T^{1/4}) \quad \text{Equation 5.5}$$

where C and D are constants.

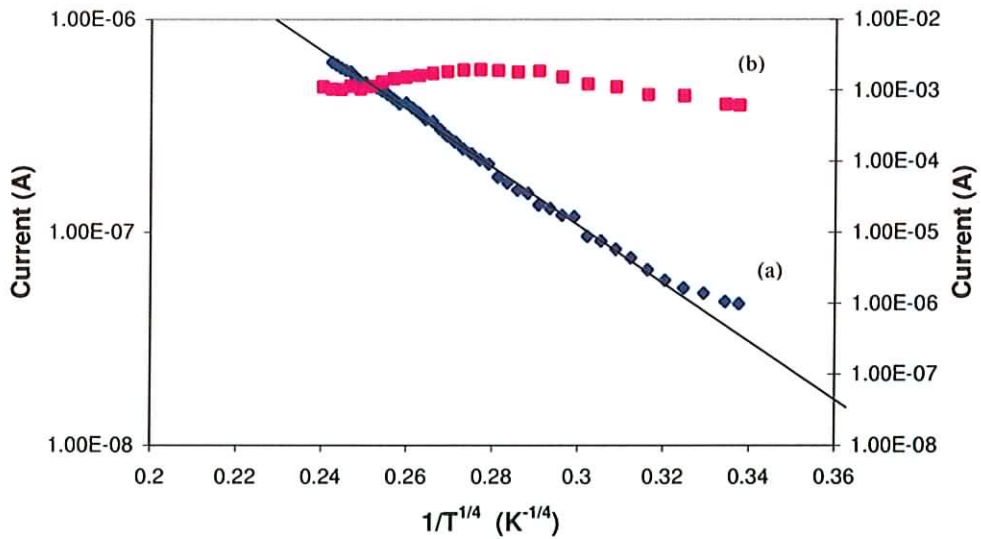


Figure 5.2: Plot of $\log I$ versus $1/T^{1/4}$ for variable range hopping. (b) plotted on x and secondary y axes, and (a), plotted on x and y axes.

Figure 5.2 plots the constant voltage current for the films produced using the two deposition rates as in Figure 5.1 in a variable range hopping format. The relatively good fit over the entire temperature range supports the theory that the electron hopping is variable and not fully a well defined thermally activated hopping state. This $T^{1/4}$ temperature dependence is typical of non-crystalline molecular solids.

In both Figure 5.1(b) and Figure 5.2(b) it is seen that the current seems to remain approximately constant which suggests that the conductivity for this film is independent of temperature. In Figure 5.1 (a) however the current varies over at least an order of magnitude, whereas in Figure 5.1(b) the variation over the temperature range is significantly less than an order of magnitude. This implies that transport becomes less reliant on thermal activation and there is a greater intermolecular delocalisation of electrons. Such behaviour has previously been observed in annealed fullerene films where an insulator to metal transition has occurred. The similarities here give further support to the proposal that the films produced via a slow deposition rate are at least partially annealed.

5.3 Current Voltage Characteristics

Figure 5.3 shows the IV curves for films produced using the three different boats all taken at room temperature. The three films tested were of similar thicknesses of the order of 580 nm. It is immediately apparent that the three films have very different resistivities (or conductivities). The conductivities (σ) can be calculated by using equation 3.1 to be:

Boat 1	slope = 0.0148	$\sigma = 1.81 \times 10^{-6} \text{ S cm}^{-1}$
Boat 2	slope = 0.0028	$\sigma = 2.92 \times 10^{-7} \text{ S cm}^{-1}$
Boat 3	slope = 0.001	$\sigma = 1.21 \times 10^{-7} \text{ S cm}^{-1}$

The first boat used yielded films of conductivity substantially higher than typically quoted for polycrystalline fullerene films [4]. Elevated conductivity implies that the films are not of pristine quality, as pristine C_{60} should result in insulator type characteristics. The elevated conductivity is similar to the increased conductivity observed in annealed fullerene films and is consistent with the relative temperature independence of Figure 5.1(b). From the absorption spectra of Chapter 4, it was deduced that the films produced using boat 1 were annealed to some extent. The electronic characteristic of the films supports this proposal. These conductivities above were calculated linearly from Figure 5.3. However on closer examination it was seen that the IV characteristic obtained from boat 3 (Figure 5.4) deviated from the linear behaviour resulting in two conductivities as described below.

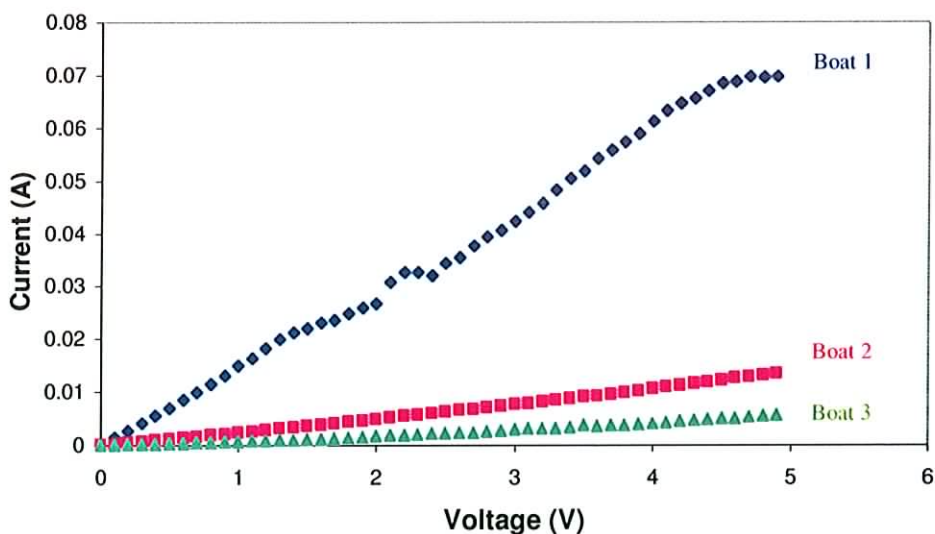


Figure 5.3: IV curves obtained from the three different boats

The conductivity of the films produced at fast deposition rates from boat 3 exhibit a conductivities as low as $10^{-8} \text{ S cm}^{-1}$ which is much more characteristic of pristine fullerene films. The activated behaviour of Figure 5.1(a), as well as the absorption spectra of Chapter 4 further supports the proposal that under these conditions, a fast deposition rate is desirable to produce thin films of pristine C_{60} .

It should be noted that although the behaviour of the IV curve (boat 3) appears linear, there is significant deviation from Ohmic behaviour, as shown in Figure 5.4. This shows the characteristic IV of a film 580 nm thick with an area of 0.48 cm^2 . Initially the slope is approximately 5.8×10^{-4} which yields a conductivity of $7.1 \times 10^{-8} \text{ S cm}^{-1}$, as the voltage increases the conductivity also increases to $1.9 \times 10^{-7} \text{ S cm}^{-1}$, determined from the second half of the graph, with a slope of $\sim 1.6 \times 10^{-3}$.

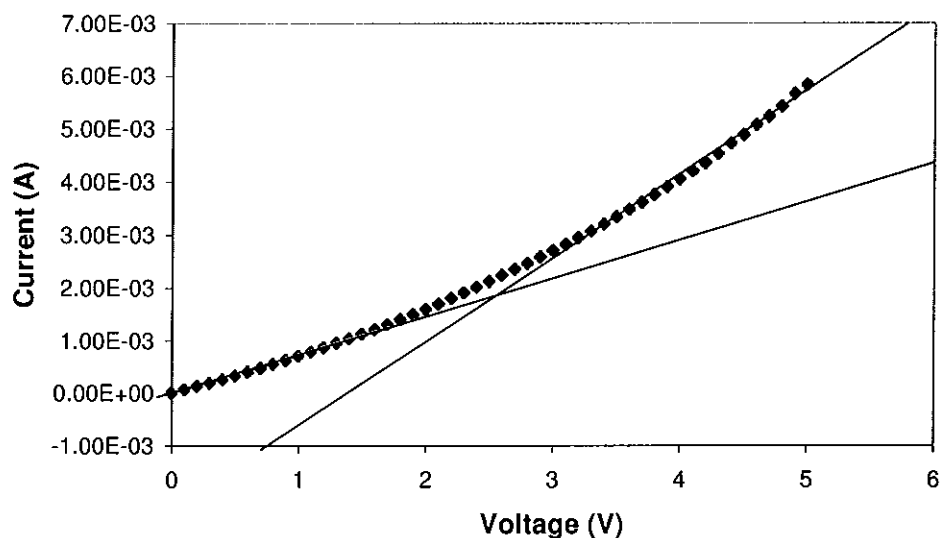


Figure 5.4 Current-Voltage characteristic of a 580 nm film from boat 3 at room temperature

Knowing the conductivity of the films the carrier mobility could be calculated from the equation.

$$\sigma = ne\mu \quad \text{Equation 5.6}$$

where σ is the conductivity, n is the carrier density, e is the charge on the electron and μ is the mobility. However, previous reports have shown that electroluminescence in thin films occurs sporadically in localised areas [7]. This suggests that the carrier density varies over the film and so the transport and therefore mobility are not uniform and a calculation based on external current is not valid. In order to get a real understanding of the processes involved a few conduction mechanisms should be looked at.

5.4 Conduction Mechanisms

The non-linearity of the I-V characteristics from the faster deposition boats indicates that the prevalent conduction mechanism is non-ohmic in nature. There are many different types of conduction mechanisms, which give rise to non-linear characteristics. One can explain the observed non-linearity in terms of Richardson-Schottky or Poole-Frenkel type of conduction mechanisms.

5.4.1 Richardson-Schottky emission

Schottky [11] emission occurs due to thermal activation of electrons over the metal-insulator or metal-semiconductor interface barrier because of lowering of barrier height due to the applied field. One of the most interesting properties of any metal-

semiconductor (MS) interface is its Schottky barrier height (SBH). The SBH is the rectifying barrier for electrical conduction across the MS junction and, therefore, is of vital importance to the successful operation of any semiconductor device. The magnitude of the SBH reflects the mismatch in the energy position of the majority carrier band edge of the semiconductor and the metal Fermi level across the MS interface. At a metal/n-type semiconductor interface, the SBH is the difference between the conduction band minimum and the Fermi level. For a p-type interface, the SBH is the difference between the valence band maximum of the semiconductor and the metal Fermi level.

5.4.2 Poole-Frenkel effect

The Poole-Frenkel [12] effect is basically similar to the Schottky effect, except that it is applied to thermal excitation of electrons from traps into the conduction band of the insulator.

In both the above cases the $\log I$ versus $V^{1/2}$ characteristics are expected to be linear in nature. When plotted, if it is seen that the characteristic curve is still non-linear in nature, then this would rule out the possible existence of Richardson Schottky or Poole-Frenkel as the sole conduction mechanisms of the system.

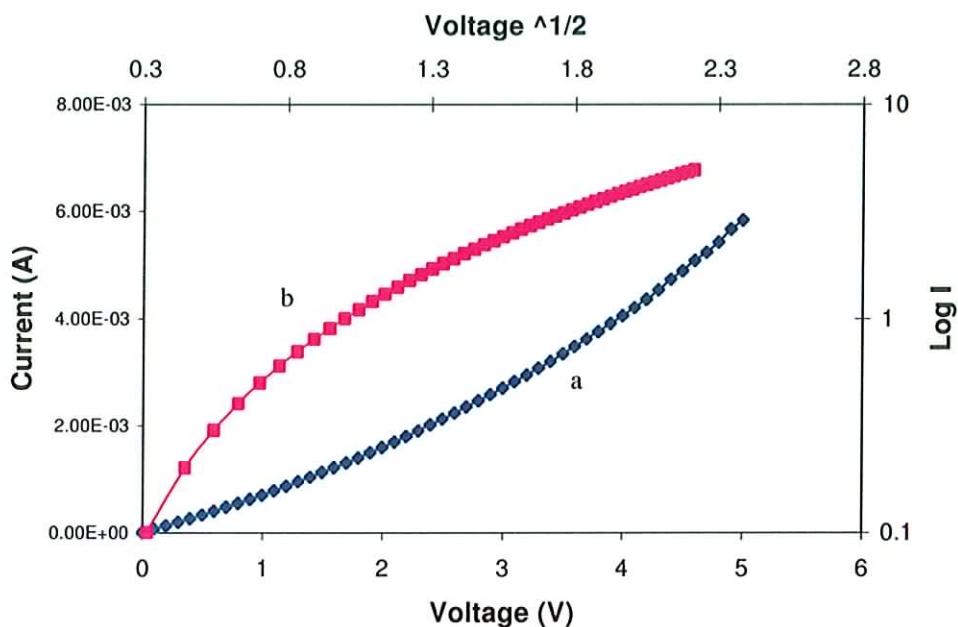


Figure 5.5: Room temperature I-V. curve a, and $\log I$ vs. $V^{1/2}$, curve b, characteristics

Figure 5.5 shows the current voltage characteristics of film 580 nm thick plotted in both I-V and $\log I$ - $V^{1/2}$ format. It is clear that the latter format does not produce a linear representation thus ruling out the above-mentioned contributions as the sole mechanism to the conduction processes.

5.4.3 Space charge limited conduction

The third type of mechanism that gives rise to highly non-linear I-V characteristics is the space charge limited conduction (SCLC) [13]. It is the traps in the lattice structure of the material that contribute to this type of conduction mechanism. However, the exact nature of the traps present in the material under study depends on both the type of traps present and their position with respect to the Fermi-level. In the case of fullerenes,

each molecule in the lattice can, in a way, be considered as a trap. Electrons on the outer shell of the molecules need energy to be able to move from one molecule to the other. Hence it can be assumed that the electrons are essentially trapped until they receive the required amount of energy. It is necessary to apply this theory very carefully to explain experimental results. Since vacuum evaporated films tend to be a mixture of amorphous and crystalline regions, it can be expected that a large concentration of traps distributed in the energy band gap may be present [13]. Therefore, the SCLC phenomenon appropriate to such a distribution can be applied to describe the condition of these films. As the exact distribution of traps is difficult to predict, an approximation to the real distribution could be attempted.

5.5 High Voltage transport

Although the electronic analysis was done at relatively low voltages it can be concluded from the graphs above that the electronic properties of solid-state fullerenes are strongly dependent on the deposition rate. A high voltage analysis yields more interesting results shown in Figure 5.6. As described in the introduction, studies have shown that with pristine films the sample is seen to start off weakly conducting and almost “jump” into a highly conducting state [7]. The inability to reproduce this behaviour routinely prompted the study of the deposition methods described in the preceding chapters.

The IV depicted in Figure 5.6 was obtained for a film of 580 nm at room temperature at a fast deposition rate (from boat 3). The IV characteristics at elevated voltages indicates an increase in conductivity with increasing voltage with a broad maximum in conduction followed by an abrupt decrease in the conductivity. The abrupt decrease in

conductance is consistent with what has been observed in pristine fullerene films (Figure 1.4) and has been ascribed to a collapse of the fullerene lattice at high charge densities [14]. After the subsequent drop in conductivity the film was then rerun through the same voltage range. The graph obtained did not follow the same trend as that of the above which confirms that there was a change in the lattice structure. Although the nature of the change is not fully characterised it has been suggested that this structural collapse is due to the instability of the C_{60} lattice to the addition of electrons. As briefly stated in Chapter 1, Smie and Heinze described this process as a dimerisation of the lattice at ~50% charging such that the added charge is shared by two molecules. The secondary peak in the IV curve is thus ascribed to a further charging of the $[(C_{60})_2]^-$ species. Such a lattice reorganisation is similar to that which occurs upon photopolymerisation [15].

The onset of the increased conductance is not abrupt, however. In pristine films, the abrupt onset of high conductance has been ascribed to a space filling of traps (molecular charging), whereby at a critical charge density an insulator to metal phase transition is affected. The role of percolation in establishing such a threshold should be considered. In such a mechanism, the low conductivity of the molecularly insulating material lends itself naturally to a build up of charge density. The relatively high conductivities of even the films produced by high deposition rates implies that such a build up of charge is not achieved, there is no percolation threshold and thus no abrupt increase in the film conductance. The behaviour of Figure 5.6 is similar to that observed for annealed films implying that even at these high deposition rates the inherent conductivities of the films is too high to reproduce the previously observed nonlinear transport phenomena.

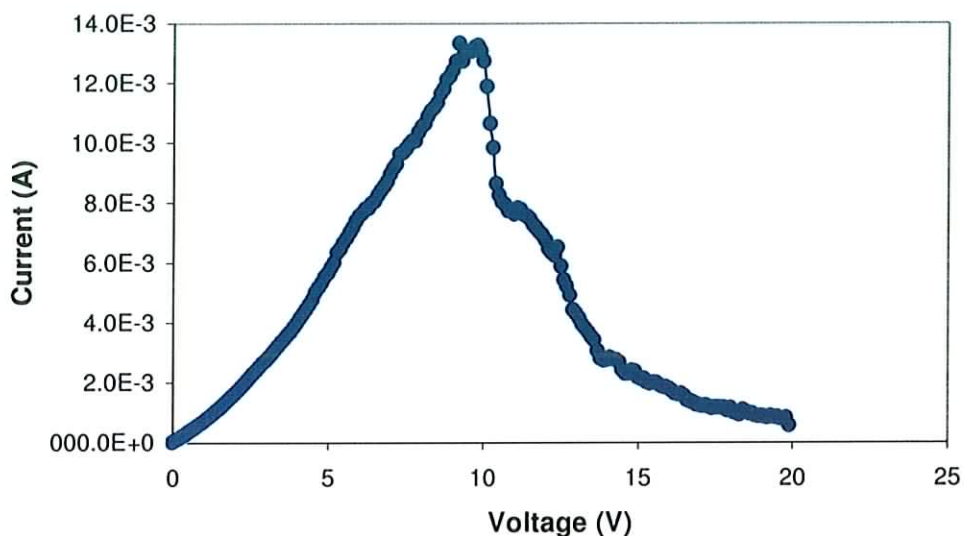


Figure 5.6: High voltage IV of C_{60} film at room temperature

There are several reasons for believing that the observed conductivity in thin insulating films is often due to extrinsic, rather than intrinsic carriers. The source of the extrinsic conductivity is thought to be the inherent defect nature of the evaporated films [16, 17]. A further problem that arises is the contamination of the films by residual gases and also by deposits arising from sublimation of other materials from the evaporation boat. Another important issue to be considered in thin films is the presence of traps in the lattice. Insulating films deposited on amorphous (glass) substrates are usually at best polycrystalline, and in many cases amorphous. For crystallite sizes of 100 angstroms trapping densities as high as 10^{18} cm^{-3} are possible because of grain boundary defects alone.

5.6 Summary

The spectroscopic study in the previous chapter illustrated that more reproducible morphologies can be produced at faster deposition rates. This chapter has shown that the deposition rate plays an important role in the electronic processes of C₆₀ thin films. A study of the temperature dependence of the conduction showed that films produced by high deposition rates exhibit a thermally activated hopping behaviour, although it appears that the observed behaviour is better described by a variable range model rather than a single activated step. In films produced by slow deposition rates, the conductance is relatively temperature independent, more characteristic of annealed films. Current-Voltage characteristics showed films from boat 1 to be Ohmic in nature whereas the larger boat areas deviated from this behaviour implying that different conduction mechanisms may be dominant. It was shown that the conduction of these faster deposited films was not dominated by such mechanisms as Poole-Frenkel or Schottky emissions. It can therefore be deduced that space charge limited conduction was the major conduction mechanism involved. Ultimately a high conducting state for the C₆₀ film was achieved. A further increase in the voltage however resulted in a structural collapse showing the relative instability of the conduction state of solid C₆₀.

References

1. N. Tea, R. Yu, M. Salamon, D. Lorents, R. Malhotra and R. Ruoff, *Appl Phys A: Mat Sci*, 56, 219 (1993)
2. S. Roth and D. Carroll, *One Dimensional Metals*, Wiley-VCH (2004)

3. K. Abich, A. Keil, D. Reiss, C. Wunderlich, W. Neuhauserv and P. Toschek, *J. Opt. B: Quantum Semiclass. Opt.* 6, 18 (2004)
4. M. Kaiser, W.K. Maser, H.J. Byrne, A. Mittelbach and S. Roth, *Solid State Commun.*, 87, 281 (1993)
5. B. Pevzner, A. Hebard and M. Dresselhaus, *Phys. Rev. B* 55, 16439 (1997)
6. G. Bublitz, S. Boxer, *Annu. Rev. Phys. Chem.* 48, 213 (1997)
7. S. Phelan, PhD Dissertation, Dublin Institute of Technology (2004)
8. Cutnell and Johnson, *Physics*, 7th edition, Wiley and sons (2006)
9. K. Biljakovic, A. Smontara, D. Staresinic, D. Pajic, M. Kozlov, M. Hirabayashi, M. Tokumoto and H. Ihara, *J. Phys.: Condens. Matt.* 8, 27 (1996)
10. K. Horiuchi, S. Uchino, S. Hashii, A. Hashimoto, T. Kato, T. Sasaki, N. Aoki and Y. Ochiai, *Appl. Phys. Lett.* 85, 1987 (2004)
11. W.Z. Schottky, *Physics* 15, 872 (1914).
12. J. Frenkel, *J. Phys. Rev.* 54, 647 (1938).
13. J.G. Simmon, *J. Phys. D*, 4, 613 (1971).
14. A. Smie and J. Heizne, *Physics and Chemistry of Fullerenes and Derivatives*, World Scientific Singapore (1995)
15. A.M. Rao, P. Zhou, K.A. Wang and P.C. Eklund. *Science*, 259, 955. (1993)
16. J. Simmons, *Phys. Rev.* 155, 657 (1967)
17. J. Simmons, *J. Appl. Phys.* 18, 269 (1967)

Chapter 6

CONCLUSIONS

Conclusions

In this study the emphasis has been on exploring the dependence of optical properties and electronic conduction mechanisms in thin films of C_{60} on production methods. Many fascinating phenomena have been reported in solid state fullerenes, but their relative irreproducibility has pointed to a strong dependence on morphology. As a molecular solid, the solid state properties depend critically on the intermolecular communication. The lattice is bound by weak intermolecular forces and any small perturbations can disturb the packing.

In perfect single crystals, the intermolecular interaction varies with temperature and is abruptly affected by the rotational phase transition at 249K [1,2]. Upon illumination the molecules polymerise to form an insoluble solid. A similar material can be produced under high pressures or by thermal annealing. The presence of oxygen in the lattice can strongly affect the photophysical and electronic properties. In polycrystalline thin films, the solid state properties are inherently more variable and thus it is perhaps not surprising that many observations on the electronic and optical properties suffer from poor reproducibility. During the course of this study it was seen that the correlation between the absorption and thickness of the films did not coincide with that of the Lambert Beer law. This was intriguing and so the production method of the films was observed as to ascertain the parameters that govern the morphology of the films.

The most obvious parameters that could affect the film growth are deposition time and substrate distance. In order to perform a qualitative study of the deposition rate, the substrate distance was kept at a maximum (~15 cm) and the deposition rate was varied.

The variation of the deposition rate involved the utilisation of evaporation boats of different areas, the smaller the area the slower the deposition rate. It is known that the electronic properties of solid-state fullerenes are critically dependent on the local environment and crystal packing. This proposes intriguing questions as to the morphology of the films and the reproducibility in creating films of identical or even similar morphologies.

In order to ascertain the answers to many of the questions that have been posed the experimental analysis utilised different parameters. A spectroscopic study was conducted using the UV-Vis spectrometer. However this yielded results, which in turn posed yet more questions. The morphologies of the films seemed irreproducible and so the crystallinity of the films needed to be improved so as not to hinder the spectroscopic properties. It was later observed that the larger boat area, or faster deposition, produced more reproducible absorption spectra, which implied that the films themselves were of similar morphologies. Electronic analysis of the films also showed that the faster deposited films produced lower conductivities comparable to that of pristine C_{60} .

Conduction in thin films can be dominated by many mechanisms like Richardson-Schottky emissions and the Poole-Frenkel effect. In This study it was shown that neither of these were the sole conduction mechanisms and so it could be deduced that space charge limited conduction also played a role in the conductivity of the films. This mechanism infers that each of the molecules within the lattice can be thought of as individual traps. The electrons have to acquire enough energy to be able to move from one molecule to the next, thus creating a conduction path. The final result yielded a film that at relatively high voltages was seen to become highly conducting. As C_{60} is

known to be a molecular insulator, this high conductivity suggested that an insulator to metal-like transition may have occurred.

This study has shown that the boat size plays a larger part in the production process of C₆₀ thin films. Evaporation of molecular materials can be very intricate in that many stresses and defects may be introduced into the lattice during this process. As mentioned previously there are many factors that may affect the morphology and hence the conductivity of the films. Some experiments that have been carried out strongly suggest that oxygen affects the transport properties of fullerene films in at least two ways [3]. In the initial few minutes of exposure oxygen diffuses along the grain boundaries, which can rapidly decrease the conductivity by a few orders of magnitude. Then over a few hours the oxygen can diffuse into the grains lowering the conductivity yet again by a few more orders of magnitude [4]. It is evident that the crystalline structure of the fullerene films may strongly affect this diffusion process.

References

1. J. Fisher, P. Heiney, D. Luzzi and D. Cox, *Fullerenes: Synthesis, Properties and Chemistry of Large Carbon Clusters*, American Chemical Society Symposium Series 481, 55 (1992)
2. H. Kuzmany, M. Matus, B. Burger, J. Winter, *Adv. Mater.* 10, 731-745. (1994)
3. B. Pevzner, A. Hebard and M. Dresselhaus, *Phys. Rev. B* 55, 16439 (1997)
4. D. Han, H. Habuchi, S. Nitta, *Phys. Rev. B* 57, 3773 (1998)

